Establishment of a Three-dimensional (3D) *In Vitro* Model for Culture of Brown Trout (*Salmo trutta* f. *fario*) Primary Hepatocyte Spheroids - Insights into 5alpha-Dihydrostestosterone Regulation of Lipid-Related Genes
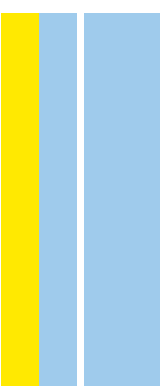
Inês Lopes Pereira

M

2019

U.PORTO

M.FCUP 2019

INÊS LOPES PEREIRA

Establishment of a Three-Dimensional (3D) *In vitro* Model for Culture of Brown Trout (*Salmo trutta* f. f*ario*) Primary Hepatocyte Spheroids – Insights into 5α-Dihydrotestosterone Regulation of Lipid-Related Genes

Dissertation for the master's degree in Environmental Contamination and Toxicology, submitted to the Institute of Biomedical Sciences Abel Salazar of the University of Porto (U. Porto).

Supervisor – Tânia Vieira Madureira
Category – Auxiliary Researcher and Invited Auxiliary Professor
Affiliation – Interdisciplinary Centre of Marine and Environmental Research (CIIMAR/CIMAR), U. Porto, and Institute of Biomedical Sciences Abel Salazar, U. Porto

Co-supervisor – Eduardo Jorge Sousa da Rocha
Category – Full Professor
Affiliation – Institute of Biomedical Sciences Abel Salazar, U. Porto, and Interdisciplinary Centre of Marine and Environmental Research (CIIMAR/CIMAR), U. Porto

Acknowledgements

To Professor Tânia V. Madureira, my supervisor, I would like to thank for all the support, help, guidance and availability during my Master thesis.

To, Professor Doctor Eduardo Rocha my co-supervisor, I need to thank for all the guidance along this journey.

I would like to thank to PhD student Célia Lopes for the teachings, patience and for all the time spent helping me.

To PhD student Fernanda Malhão and lab technician Paula Teixeira, I would to thank for the help and patience during my work in the laboratory.

I would like to thank to my mum and dad for all the constant support and for making this master's possible. To my sister for the company and for never keeping her feet on the ground. To all my family for the support and good times.

I would like to thank to all my friends and their support along this journey. Specially to Maria for the company, to Ana Macedo, Anette and Inês D.

I would like to thank to Kostadin, without whom this thesis would not be finished. And for having a colony of snails.

Abstract

Three-dimensional (3D) culture models have been recently developed for ecotoxicological testing, since these systems reflect *in vivo* conditions of the cells in their native environments. The goal of this project was to establish a novel 3D system for culture of primary hepatocyte spheroids obtained from juvenile brown trouts. In addition, this research aims to provide new insights into androgenic metabolic signalling, essentially, to uncover the influence of 5α-Dihydrotestosterone (5α-DHT) on lipid metabolism-related genes. Sex steroid hormones are known to display important regulatory roles on lipid pathways, with consequences for energy homeostasis in the liver. Most literature reflects the effects of estrogenic compounds on fish reproductive physiology, with limited research on androgens.

The optimization of culture conditions for growth of spheroids was carried out by testing three different culture media. Characterization of the spheroids was performed by assessing cellular viability (tetrazolium salt and resazurin reduction), biometry (equivalent diameter, sphericity, area and volume) and morphology. The optimal medium was identified as DMEM/F-12 medium with 10% (v/v) FBS, 15mM of HEPES and 10 mL/L of antibiotic/antimycotic solution at 18 ºC, without additional supply of O_2/CO_2, and at a constant agitation of ±100 rpm. According to the biometric parameters and to histological evaluations, we confirm that spheroids acquired morphological maturity from the 6 - 8th day post-isolation, and were maintained viable until 30 days in culture.

Molecular analysis of 2D exposures to six concentrations of 5α-DHT (1 nM, 10 nM, 100 nM and 1 µM, 10 µM, 100 µM) showed a tendency to increase the mRNA *Fabp1* levels after exposure to the highest 5α-DHT dose. *ApoAI* mRNA levels were not altered. *Acsl1* was significantly up-regulated following exposures to 1 µM, 10 µM and 100 µM of 5α-DHT. *Acox1-3I* and *PPARγ* mRNA levels were not altered. 3D exposures to 5α-DHT (at 10 and 100 µM), under the optimized test conditions, caused altered gene expressions in four lipidic target genes. A down-regulation was observed for *Acox1-3I* and *PPARγ*, following exposure to 100 µM of 5α-DHT. On the contrary, *Acsl1* was up-regulated after exposure to both 5α-DHT concentrations, and up-regulation of *Fabp1* mRNA levels were also noted, but only for the highest dose. *ApoAI* mRNA levels displayed no alterations. These results demonstrated that, at the same doses, brown trout hepatocytes cultured in 2D were affected to a lesser extent than hepatocytes in 3D, although a similar tendency was noted in gene expression. Thus, testing models closer to *in vivo* is of uttermost importance, as otherwise the effects may be underestimated. Further, the present data is

extremely relevant to reinforce the importance of the study of androgenic compounds in lipid metabolic pathways in fish and infer their physiological consequences.

Resumo

Os modelos de culturas tridimensionais (3D) têm sido desenvolvidos para testes ecotoxicológicos uma vez que estes reflectem as condições *in vivo* nos ambientes naturais das células. Um dos objectivos deste projecto consistia em estabelecer um sistema 3D para culturas de esferóides de hepatócitos primários da truta fário (organismo-modelo). Adicionalmente, este trabalho pretende estudar a sinalização metabólica mediada por andrógenos, especificamente, a influência da 5α-DHT nos genes relacionados com o metabolismo lipídico. As hormonas esteróides sexuais têm um papel importante na regulação de vias lipídicas, com impacto na homeostasia energética hepática. A literatura existente foca-se maioritariamente nos efeitos de compostos estrogénicos na fisiologia reprodutiva de peixes, existindo poucos estudos relativos a androgénios. A optimização das condições de cultura para o crescimento dos esferóides foi executa utilizando três meios de cultura diferentes. A caracterização dos esferóides foi feita através de ensaios de viabilidade (redução de sais de tetrazólio e resazurina), biometria (diâmetro equivalente, esfericidade, área e volume) e morfologia. Foi concluído que o meio óptimo é DMEM/F-12, com 10% (v/v) FBS, 15mM of HEPES e 10 mL/L de solução antibiótica/antimicótica a 18 ºC, sem adição de O_2/CO_2, e com uma agitação constante de ±100 rpm. Os esferóides atingiram a maturidade morfológica por volta do 6º - 8º dia após o isolamento de células e foram mantidos viáveis durante 30 dias em cultura.

A análise molecular das exposições bidimensionais (2D) a seis concentrações de 5α-DHT (1 nM, 10 nM, 100 nM e 1 µM, 10 µM, 100 µM) indicou uma tendência por parte dos níveis de mRNA de *Fabp1* a aumentar após a exposição à concentração mais elevada de 5α-DHT. A expressão genética de *ApoAI* não foi alterada. Verificou-se um aumento da expressão genética de *Acsl1* após a exposição a 1 µM, 10 µM e 100 µM de 5α-DHT. Os níveis de mRNA de *Acox1-3I* e *PPARγ* não sofreram alterações neste modelo. Exposições 3D a 5α-DHT (a 10 e 100 µM), nas condições optimizadas, causaram alteração na expressão genética em quatro dos genes lipídicos testado. Após a exposição a 100 µM de 5α-DHT, foi observada uma diminuição de expressão genética dos genes *Acox1-3I* e *PPARγ*. Por outro lado, os níveis de mRNA de *Acsl1* aumentaram após a exposição a ambas as concentrações de 5α-DHT, e para a concentração mais elevada, também foi observado um aumento da expressão de *Fabp1*.

Os níveis de mRNA da *ApoAI* não sofreram alterações. Estes resultados demonstraram que, para as mesmas doses, os hepatócitos de trutas fário em culturas 2D foram menos afetados que os das culturas 3D, apesar de ter sido observada uma tendência semelhante na expressão genética. Deste modo, a realização de testes com modelos que melhor reproduzam as condições *in vivo* é de extrema importância, visto que, de outra forma, os efeitos podem ser subestimados. Os dados apresentados revestem-se de extrema relevância, uma vez que reforçam a importância do estudo de compostos androgénicos nas vias metabólicas lipídicas nos peixes e as suas consequências biológicas.

Table of Contents

List of Figures

List of Tables

Chapter 1. Introduction

1.1 Lipids and Lipid Pathways in Fish - Main Aspects

Lipids are vital biomolecules that constitute the building blocks of essential cellular components. Characterized by their solubility in non-polar solvents, lipids are composed of fatty acids (FA), usually linked to different chemical groups. In fish, lipids and proteins are the primary nutritional and energy sources, while carbohydrates are used in minor amounts (Sargent *et al.*, 2003). Lipids can either be acquired through the diet or synthesized from acetyl-coA in the organism. These molecules can be classified according to their polarity: non-polar lipids are insoluble in water and comprise mono-, di- and triglycerides (TG), esters of fatty acids and glycerol; sterol esters, like cholesterol; wax esters or sphingolipids, esters with the sphingosine amino group. Phospholipids, contain polar groups in their structure and are the main component of cellular membranes, therefore displaying significant roles in cellular structure and integrity (Arts & Kohler, 2009; Tocher, 2003).

Living cells rely on lipids for: (1) the supply of essential FA from diet; (2) the generation of energy through catabolic reactions; (3) long-term energy storage in the adipose tissue, as well as, in the biosynthesis of hormones and bile acids from cholesterol. Additionally, lipids can function as enzyme co-factors, and as precursors to several molecules, such as vitamins or eicosanoid metabolites (Leaver *et al.*, 2008; Turchini *et al.*, 2009). An important physiological and regulatory feature is their ability to act as signalling molecules in different vital pathways, either by the activation of cascades or specific nuclear receptors. Thus, maintenance of lipid homeostasis is crucial for normal growth and development, organ physiology, gonadal maturation, metabolism, and reproduction in fish (Higgs & Dong, 2000; Madureira *et al.*, 2018; Turchini *et al.*, 2009).

The liver is the major site of lipid metabolism, where the rate-limiting enzymes for fatty acid oxidation and lipogenesis are located. It is also the site where biosynthesis of n-6 and n-3 long chain polyunsaturated fatty acids (PUFAs), eicosapentaenoic acid (EPA; 20:5n-3), docosahexaenoic acid (DHA; 22:6n-3) occurs (Monroig *et al.*, 2018). These are essential nutritional requirements in all vertebrates species, with important reproductive, structural and physiological functions, such as, cell signalling (Leaver et al., 2008; M. T. Nakamura & Nara, 2004; Sargent et al., 2003). In addition, PUFA and long-chain PUFA are the major components of cellular membranes, influencing its composition (Higgs & Dong, 2000).

Digestion of lipids generates free fatty acids (FFA) that must be distributed throughout the body, in order to exert their functions. Lipids can be transported into muscles and tissues for energy supply, into adipose tissue for energy storage and, eventually, returned into the liver, either to be recycled or excreted. However, due to their insolubility in water, transportation of lipids via the lymphatic and circulatory systems depends on the formation of lipoproteins, comprising a hydrophobic core with cholesterol and triglycerides surrounded by hydrophilic phospholipids and apolipoproteins (Tocher, 2003). Lipoproteins can be classified according to lipid content and density. Chylomicrons (CM) are produced in intestinal cells from the absorption of lipids, while very low density lipoproteins (VLDL) are generated in the liver, both contain high amounts of triglycerides and low percentages of cholesterol. However, facilitation of the lipoprotein's content into cells is necessary, and must be achieved by TG's hydrolysis by lipoprotein lipase (LPL). The break of ester bonds leads to FA's release and formation of intermediate-density lipoproteins (IDL) (José Ibáñez *et al.*, 2008; Tocher, 2003) In turn, low density lipoproteins (LDL) have low triglyceride content and the highest levels of cholesterol amongst lipoproteins. Thus, the delivery of cholesterol to cells and to the liver is accomplished by LDL. High density lipoproteins (HDL) contain mostly proteins with low levels of lipids, hence entering the circulatory system for collection of excess cholesterol from tissues and transportation into the liver for uptake. The structure and composition of lipoproteins are similar across vertebrates (including some variations of lipid composition according to the fish species).Besides, the pathways involved in lipid metabolism and transport occur in similar manners in fish and mammals (Zheng *et al.*, 2013). Notwithstanding, differences do exist, being HDL the lipoprotein present in higher amounts in the blood of salmonids, as opposed to VLDL and HDL in mammalians, for instance (Tocher, 2003; Turchini *et al.*, 2009).

There are major pathways and processes involved in lipid metabolism. The liver is a major site of lipogenesis (lipid biosynthesis from acetyl-CoA) and lipolysis (hydrolysis of triglycerides). Following lipolysis, β-oxidation involves the conversion of acyl-coenzyme A (acyl-CoA) esters into the corresponding 2-trans-enoyl-CoA esters. It might occur in the peroxisomes or in the mitochondria, being the latter a main source of energy. These steps are similar in mammalian and fish species (Ayisi *et al.*, 2018; Cunha *et al.*, 2013; He *et al.*, 2015; Madureira *et al.*, 2016a).

1.2 Sex Steroid Hormones as Regulators of Lipid Metabolism

Maintenance of lipid homeostasis is hormone-modulated, with androgenic and estrogenic sex steroid hormones playing pivotal roles. Steroidogenesis is the production of sex steroids form cholesterol in the gonads, interrenal gland or in the brain (Shen & Shi, 2015; Tokarz *et al.*, 2015). In vertebrates, sex steroid hormones exert their regulative actions through Androgen (AR), Estrogen (ER) or Progesterone (PR) receptors that belong to the nuclear receptor superfamily. These consist in ligand-dependent transcriptional regulators, that control the transcription of tissue specific target genes when activated. Regulation of lipid metabolism is essential for energy production, organ physiology and reproduction (Borg, 1994; Young *et al.*, 2005; Zhao *et al.*, 2015). Therefore, deregulations of these pathways have been linked to obesity-mediated metabolic diseases or other pathologies or conditions (Mayes & Watson, 2004; Velasco-santamaría *et al.*, 2011).

1.2.1 Androgenic Hormones

The major circulating androgens in mammals are Testosterone (T) and 5α-Dihydrotestosterone (5α-DHT), critical for the development of male reproductive system. Testosterone is the most important and studied androgen. It can be converted into more potent androgens, in 5α-DHT by 5α-reductase in the peripheral tissues, or into 11-Ketotestosterone (11-KT) by Cytochrome P450 and 11-βhydroxysteroid dehydrogenases in the inter-renal tissue (Borg, 1994; Imamichi *et al.*, 2016). Contrasting with its precursor hormone, 5α-DHT is a non-aromatizable androgen, which means it can't be converted into estradiol in steroidogenesis. 11-KT was identified with higher concentrations in the plasma of teleost fishes and humans. The latter is considered to be the most potent androgen in fish (Divers *et al.*, 2010; Imamichi *et al.*, 2016; Matsumoto *et al.*, 2013).

The AR is the main mechanism through which androgenic compounds, endogenous or synthetic, control lipidic pathways. Effects at the molecular level result from the binding of an activated AR to an androgen response element in the target genes. However, AR-independent mechanisms of androgenic signalling, with non-genomic actions, are also verified (Matsumoto *et al.*, 2013).

Studies regarding the effects and roles of 11-KT in fish focus essentially on its influence on lipid-transporters, in lipoprotein lipase and in fatty acid uptake into the growing ovary of teleosts: 11-KT induced significant accumulation of lipid droplets in eels' oocytes (Endo *et al.*, 2011), as well as up-regulation of lipoprotein encoding genes (Forbes & Lokman, 2011). In humans, influence of 5α-DHT in PPAR signalling was verified, with down-regulation of *PPARα* (Collett *et al.*, 2000) and *PPARγ* (Olokpa *et al.*,

2016) mRNA levels. Furthermore, in the latter work, the *PPARγ* down-regulation observed was AR-mediated in prostate cancer. In mouse pre-adipocytes and pluripotent cells, 5α-DHT exposures showed AR activation, supressed *PPARγ* expression and adipocyte differentiation (Singh *et al.*, 2003). In primary brown trout hepatocytes exposed to both estrogenic and androgenic stimuli, *PPARγ* mRNA levels decreased, suggesting interconnection with ER and AR (Lopes *et al.,* 2016). In addition, Testosterone exposures lead to down-regulation of *PPARγ* and an up-regulation of vitellogenin A expressions (Lopes *et al.,* 2017). The results from these studies revealed important features of androgenic signalling, indicating cross-relations with peroxisomal,estrogenic and androgenic pathways. Overall, suppression of PPAR encoding genes following estrogenic and androgenic inputs suggested interference of sex steroid hormonal signalling with major lipid metabolism enzymes (Hultman et al., 2019a; Madureira et al., 2017; Singh et al., 2003). In comparison to T and 11-KT, data on 5α-DHT signalling in fish is limited, with current gaps on the knowledge of its physiological effects.

1.3 *In vitro* **Systems**

Ecotoxicological research depends on the utilization of animal testing for assessment of specific toxicological endpoints. Either for assessment of the toxic effects of specific compounds or for investigating a compound's bioaccumulation pattern or mode of action, development of *in vitro* techniques are extremely relevant (Rehberger *et al.*, 2018). One of the advantages of these systems is the possibility of large-scale screening, for example, of environmental toxicants. In comparison to animal testing, the employment of 2D systems is cheaper, allows short- or long-term experiments, as well as, application of high throughput screening assays. In addition, the conditions on which the experiments are held are highly controlled, allowing a high reproducibility of the results. Most importantly, *in vitro* assays address the issue of reducing number of animals used for research purposes (Baron et al., 2012; Hultman et al., 2019a; Kinnberg & Toft, 2003; Sonneveld et al., 2006).

The use of *in vitro* fish cultures is well established, from cell lines to primary hepatocytes. Freshly isolated primary hepatocytes are an important asset when investigating metabolic pathways, bioaccumulation or biotransformation of compounds. These systems retain cellular and organ specific mechanisms, essential for evaluation of physiological responses, like xenobiotic clearance, for example (Fay *et al.*, 2014; Han *et al.*, 2008; Li *et al.*, 2017; Segner & Cravedi, 2001).

Despite all the stated advantages of 2D *in vitro* systems, organ-specific functions are only maintained for short periods of time, leading to loss of specific activity. Cells in their natural environment display a 3D structure, and 2D systems do not allow the maintenance of proper tissue architecture. In this case, cell-cell and cell-matrix interactions are disrupted, with loss of the mechanical organization of the cells (Walzl *et al.*, 2014) In light of these features, 3D culture systems better reflect *in vivo* conditions of the cells in their native systems. In this case, fish hepatocytes in spheroid cultures spontaneously reassemble into a 3D structure. Allowing the restoration of intercellular contacts, cell-matrix interactions, maintenance of polarity and shape (Baron et al., 2012; Hultman et al., 2019a; Uchea et al., 2015, 2013).

The use of fish 3D models has increased in recent years, with advances at the methodology level. This increase is related to a pursue of improved predictions of realistic responses (Rodd *et al.*, 2017). 3D cultures are well established for cancer, liver and intestine cell lines in humans, rats and to a lesser extend in fish (Bachmann *et al.*, 2015; Kozyra *et al.*, 2018; Messner *et al.*, 2018). Research in fish cell lines or primary hepatocytes is still very limited. The great majority of studies focus on the characterization of the spheroids' morphological and biochemical features (Baron *et al.*, 2017, 2012; Cravedi *et al.*, 1996; Flouriot *et al.*, 1993; Lammel *et al.*, 2019; Langan *et al.*, 2018; Uchea *et al.*, 2015). In addition, few works evaluate the bioaccumulation and biotransformation of pharmaceuticals in the spheroids (Hultman et al., 2019a; Uchea et al., 2013). To our knowledge only two studies have performed exposures to environmental toxicants using fish 3D liver cultures (Hultman *et al.*, 2019; Rodd *et al.*, 2017).

1.4 Aims and Objectives

In general, this project aims to develop a novel 3D system for culture of brown trout primary hepatocyte spheroids, suitable for metabolic and genetic studies, long-term applications and ecotoxicological research. This work intends to complement the scarce literature on 3D cultures from fish primary hepatocytes, since research in fish is mostly focused on spheroid cultures from cell lines, namely from liver, intestine and cancer cells. Establishment of this model would provide a viable alternative to *in vivo* testing, since it has been proved that cells in a 3D organization better reflect *in vivo* responses, and general organ functions. In addition, application of 3Rs policy was pursued, for reduction, refinement and replacement of animal testing, with a responsibility for animal welfare (4th R).

The current increase of pharmaceuticals and personal care products (PPCPs) in aquatic environments negatively impacts wildlife's physiological functioning and survival. These products may display endocrine-disrupting properties, since they mimic endogenous compounds such as hormones, affecting several physiologically relevant metabolic pathways and functions in aquatic animals (Brockmeier *et al.*, 2014; De Falco *et al.*, 2015; Milla *et al.*, 2011; Velasco-santamaría *et al.*, 2011).

This research aims to provide new insights into androgenic metabolic signaling, essentially, to uncover the influence of 5α-DHT, a model non-aromatizable androgen, on lipid metabolism-related genes. Sex steroid hormones are known to display important regulatory roles on lipid pathways, with consequences for energy homeostasis in the liver. However, studies in fish are mainly focused on estrogenic signaling mechanisms (Lopes *et al.*, 2017; Madureira *et al.*, 2015; Shen & Shi, 2015). Therefore, investigation of the lipid transcriptional targets of 5α-DHT, and the metabolic pathways involved is extremely important. Hence, treatments for pathological lipid-related conditions, as well as, understanding the endocrine disrupting chemical's (EDC) mode of action can only be improved by unveiling of such pathways (Brockmeier *et al.*, 2014; Sakkiah *et al.*, 2017).

In this work, a teleost fish model organism was used, the brown trout (S*almo trutta* f. *fario*). Teleost fishes and mammals share developmental and physiological aspects, with similarities in the functioning, composition and signaling of the endocrine system (Dickhoff *et al.*, 1990). Therefore, employment of the liver of brown trout has proven to be a suitable system for the study of hormonal regulation, enzymatic activity and genetic expression (Lopes *et al.*, 2017; Madureira *et al.*, 2016a, 2015; Rocha *et al.*, 1997). In order to achieve these goals, three main tasks have been designed.

Initially, optimization of the culture conditions for growth of 3D spheroids from brown trout primary hepatocytes is intended. Three test conditions were selected and the characterization of spheroids will be performed by assessing cellular viability, biometry and morphology.

Next, 5α-DHT exposures of 3D spheroids from brown trout primary hepatocytes are planned during 96 h. Characterization of spheroids will be accomplished using viability assays, histological staining techniques, immunohistochemistry, transmission electron microscopy (TEM) and molecular analyses.

Finally, lipid metabolism-related gene's expression from 2D monolayer and 3D spheroids of brown trout primary hepatocytes exposed to 5α-DHT will be compared. A selection of target genes from different lipid metabolism pathways will be tested: *Acsl1*, involved in FA activation into CoA esters (Cheng *et al.*, 2017; Lopes-Marques *et al.*, 2013); *Acox1-3l*, the first rate-limiting enzyme in peroxisomal oxidation in the conversion of fatty acyl-CoA esters (Madureira *et al.*, 2016a); *ApoAI*, the main component of HDL for

lipid transport (Sahoo *et al.*, 2017); *Fabp1*, for FA uptake and intracellular transport (Venkatachalam *et al.*, 2012), and the transcriptional regulatory factor *PPARγ* involved in the control of lipid metabolism (Cunha *et al.*, 2013; Kamalam *et al.*, 2013).

Chapter 2. Materials and Methods

2.1 Fish Provenance and Maintenance

Brown trout (*Salmo trutta* f. *fario*) juveniles were acquired from the Aquaculture Station of Torno, in the North of Portugal (Council of Amarante). Fish were acclimated at the Aquatic Animal Facility at ICBAS-UP, for at least 4 weeks prior to experiments, in a 1000 L tank with filtered and dechlorinated tap water. Fish were maintained in a natural photoperiod of 12 h light/12 h dark. Fish were fed daily with dry granules for salmonids (T-4 Optiline, Skretting), excepting 24 h prior to hepatocyte isolation. Sexually immature one-year-old brown trout were used in all experiments, with a mean weight of 51.67 (±14.7) g, and a total length of 16.77 (±1.6) cm. Water quality parameters were measured at least once a week, and were as follows [mean (± standard deviation)]: ammonium - 0 mg/L, ammonia - 0.003 (± 0,012) mg/L, nitrates - 38.4 (± 8.2) mg/L, nitrites - 0.15 (± 0.3) mg/L, oxygen (O_2) - 92.2 (± 2.7) %, pH - 8.3 (± 0.1), temperature - 18.4 (± 0.9) °C and total hardness (GH) - 6 (± 0.5)°dGH.

2.2 Isolation of Hepatocytes from Brown Trout

Fish were euthanized with an overdose (0.6 mL/L) of ethylene glycol monophenyl ether (Merck). The Portuguese Decree-Law No. 113/2013 implementing EU Directive No. 2010/63 on animal protection for scientific purposes was followed for all procedures involving animal handling. For 2D primary culture and exposure assays, hepatocytes were isolated from 2 immature brown trout juveniles. Regarding 3D primary spheroid cultures, hepatocytes were obtained from 3 animals at the same development stage for optimization assays, and from 2 fish for 5α-DHT exposure assay.

Primary hepatocytes were obtained through a two-step collagenase perfusion technique adapted from the isolation of mammalian hepatocytes (Lee *et al.*, 2013; Seglen, 1976), that was previously optimized for teleost fish (Segner, 1998), and ultimately for brown trout, as detailed elsewhere (Madureira *et al.*, 2015).

Buffers and Stock solutions were prepared as described in Appendix Aand filtered on the day of hepatocyte isolation, with 0.2 µm filters (GE Healthcare). Prior to liver isolation, as much blood as possible was collected from the fish with an insulin syringe (Pic solution), through a puncture on the caudal vein, followed by dissection of the animal and liver removal. Subsequently, buffer 1 (Appendix A) was used in the perfusion of the liver using a peristaltic pump (Minipuls 3 Gilson), and by inserting a plastic cannula with

an Abbocath 24G needle (100 Sterican, BBraun) in the hepatic vein(s). An initial perfusion velocity of ≈ 6.7 was applied, followed by a gradual increase, for an efficient blood removal from the liver. For tissue disaggregation, collagenase at 0.05% was added to buffer 2 (Appendix A) prior to its use, and perfusion was continued at an initial velocity of ≈ 6.7 with a gradual increase. The liver was then placed in buffer 3 (Appendix A) for mechanical dissociation and disruption. The resulting cellular suspension was filtered with 200 μm followed by 50 μm mesh size nylon membranes. Pellets were obtained after three consecutive centrifugation steps at 160 g for 5 min at 4 ºC. Finally, pellets were resuspended in the appropriate final culture medium.

2.3 Two-Dimensional (2D) Culture Experimental Design

Brown trout's primary hepatocytes from 2 immature juvenile fish were isolated and cellular suspensions were plated at a density of 1×10^6 cells/mL, in 24-well plates (SPL Life Sciences), previously coated with 300 μg/mL of poly-L-lysine (Sigma-Aldrich). Hepatocytes were cultured in 500 μL of Leibovitz's L-15 medium without phenol red (Invitrogen), supplemented with 5% charcoal-stripped fetal bovine serum - FBS (Sigma-Aldrich), 100 μg/mL of streptomycin and 100 U/mL of penicillin (Sigma-Aldrich), at 19 ºC, without additional supply of O_2/CO_2. Primary hepatocytes were exposed for 96 h to: L-15 supplemented medium (control – C); 0.1% ethanol in supplemented L-15 medium (solvent control – SC) and 6 concentrations of 5α-DHT (Sigma-Aldrich) 1, 10 and 100 nM; and 1, 10 and 100 μM (corresponding to DHT1, DHT2 and DHT3; and DHT4, DHT5 and DHT6, respectively). Stock solutions of 5α-DHT were prepared in absolute ethanol p.a. (Merck), and working solutions in supplemented L15 medium, with a final ethanol concentration of 0.1%. Medium was changed every 24 h. Each well of the 24-well microplates was considered a replicate, as it was the smallest experimental unit that could independently receive a different treatment. A total of 3 plates were used for each fish, and in each one, 2 wells were randomly assigned to a specific condition for molecular analysis testing. At the end of the exposure period, hepatocytes were trypsinized, using trypsin/EDTA, 0.05%/0.02% in phosphate buffered saline (PBS) buffer (Sigma-Aldrich), and the viability was measured in a total of 3 wells/condition. Viability was assessed using trypan blue technique (Appendix B, with the Countess™ Automated Cell Counter from Invitrogen).

2.3.1 RNA Extraction and cDNA Synthesis

On the sampling day, pellets were obtained by centrifugation at 160 g for 5 min, at 4 ºC, following freezing in liquid nitrogen, and storage at -80 ºC. A total of 6 pellets (3 for each fish) were randomly selected for molecular procedures**.** Total RNA was extracted by using an Illustra™ RNA spin Mini Isolation Kit (GE Healthcare), and the protocol was followed according to the manufacturer's instructions. Quantification and purity (λ 260/280 nm) of the isolated RNA was performed with a µDrop™ Plate (Thermo Scientific) in a Multiskan GO equipment (Thermo Fisher), with SkanIt Microplate Reader software (Thermo Scientific). For blank samples the RNase-free H_2O from the isolation kit was used. A 1% agarose gel (GRS Agarose LE, GA110 GRiSP) with GelRed (Biotium) staining was performed. Imaging was acquired in a ChemiDoc XRS+ (BioRad) with the ImageLab data analysis software (BioRad).

cDNa synthesis was carried out with an iScript™ Reverse Transcription Supermix for RT-qPCR (BioRad), for a total volume of 20 µL using 250 ng of total RNA and 4 µL of iScript RT Supermix, following the manufacturer's protocol.

2.3.2 Quantitative Real-Time Polymerase Chain Reaction (RT-qPCR)

Quantitative real-time polymerase chain reaction (RT-qPCR) was performed with a CFX Connect real-time PCR detection system, using a CFX Manager software (Bio-Rad). SYBR Green reactions consisted of: 10 µL of iQ™ SYBR® Green Supermix (Bio-Rad), 5 µL of cDNA (diluted 1:5), 200 nM of each primer and the appropriate volume of water. For Eva Green reactions 10 µL of iQ™ EVAGreen® Supermix (Bio-Rad), 5 µL of cDNA (diluted 1:5), 300 nM of each primer and the appropriate volume of water were added. No template controls were performed with RNA-free water instead of cDNA. A calibrator sample was prepared by mixing 4 randomly chosen cDNA samples in a dilution of 1:10, for inter-plate normalization. Gene expression levels were calculated according to the Pfaffl method (Pfaffl, 2001). Reference genes used were β-actin (beta-actin) and rpl8 (ribosomal protein L8), which have been preciously selected and optimized in our laboratory for this model, displaying constant expression levels under androgen exposures (Lopes *et al.*, 2017). The thermal cycling protocols for the selected target and reference genes have already been described, as detailed in Table 1. along with primer sequences.

Table 1. Primer sequences for the target genes, with annealing temperatures and amplification efficiencies

Gene	Primer Forward (5' – 3')	Primer Reverse (5' – 3')	Annealing Temperature (°C)	Amplification Efficiency (%)	Reference
β-actin	TCTGGCATCACACCTTCTAC	TTCTCCCTGTTGGCTTTGG	55.0	96.1	(Madureira *et al.*, 2017)
Rpl8	TCAGCTGAGCTTTCTTGCCAC	AGGACTGAGCTGTTCATTGCG	59.0	93.8	(Körner *et al.*, 2008)
Acox1-3I	TGTAACAAGGAGCAGTTCG	TTGCCGTGGTTTCAAGCC	56.0	96.9	(Madureira *et al.*, 2016)
Fabp1	GTCCGTCACCAACTCCTTC	GCGTCTCAACCATCTCTCC	57.0	97.7	(Madureira *et al.*, 2017)
ApoAI	ATGAAATTCCTGGCTCTTG	TACTCTTTGAACTCTGTGTC	55.0	89.9	(Madureira *et al.*, 2017)
Acsl1	CGACCAAGCCGCTATCTC	CCAACAGCCTCCACATCC	55.0	97.8	(Madureira *et al.*, 2018)
PPARγ	CGGAATAAGTGCCAGTAC	GGGTCCACATCCATAAAC	56.0	98.1	(Lopes *et al.*, 2016)

β-actin (beta-actin) , Rpl8 (ribosomal protein L8), *Acox1-3I* (acyl-coenzyme A oxidase 1 – 3I isoform), *Fabp1* (fatty acid binding protein 1), *ApoAI* (apolipoprotein A I), *Acsl1* (acyl-CoA long chain synthetase 1) and *PPARγ* (peroxisome proliferator-activated receptor gamma).

2.4 Three-Dimensional (3D) Culture Experimental Design

Spheroid cultures from brown trout primary hepatocytes were carried out for optimization of growth conditions and for testing the effects of exposure to 5α-DHT. In these experiments, one well of a 6-well plate was considered a replicate, since the cells were exposed to equal independent variability sources.

2.4.1   Optimization Assays

The cells from 3 immature fish were used in order to optimize an *in vitro* methodology for culture and maintenance of viable spheroids of brown trout primary hepatocytes. Thus, a preliminary assay was performed with the purpose of selecting the most appropriate growth medium, based on previous studies carried out with 3D hepatocyte aggregates and spheroids from different fish species and cell lines (Baron *et al.*, 2017, 2012; Cravedi *et al.*, 1996; Flouriot *et al.*, 1993; Uchea *et al.*, 2015, 2013). After hepatocyte isolation, cellular suspensions were plated at a density of 0.5×10^6 cells/mL, in four 6-well plates (Falcon, Corning), with 3 mL/well of each medium:

I.   Cells incubated in Dulbecco's modified eagle medium/nutrient mixture F-12 - DMEM/F-12 (GE Healthcare Life Sciences) with 15 mM of 4-(2-hydroxyethyl)-1-piperazineethanesulfonic acid (HEPES) (Sigma-Aldrich), 10 mL/L of antibiotic/antimycotic solution, with penicillin, streptomycin and amphotericin B (Sigma-Aldrich), and 20 mL/L of serum replacement 3 (Sigma-Aldrich), at 18

ºC, without additional supply of O_2/CO_2 and at constant agitation (±100 rpm), based on Uchea *et al.* (Uchea *et al.*, 2015).

II.   Cells incubated in DMEM/F-12 with 15 mM of HEPES, 10 mL/L of antibiotic/antimycotic solution and FBS 10% (v/v) (Sigma-Aldrich), at 18 ºC, without additional supply of O_2/CO_2 and at constant agitation (±100 rpm), as described previously for rainbow trout primary hepatocytes (Uchea *et al.*, 2013).

III.   Cells incubated in Leibovitz's L-15 medium without phenol red (Gibco, Thermo Fisher), with 10 mL/L of antibiotic/antimycotic solution and FBS 10% (v/v), at 18 ºC, without additional supply of O_2/CO_2 and at constant agitation (±100 rpm), based on Baron *et al.* (Baron *et al.*, 2017, 2012).

IV.   Cells incubated in Leibovitz's L-15 medium without phenol red with 10 mL/L of antibiotic/antimycotic solution and FBS 10% (v/v), at 18 ºC, without additional supply of O_2/CO_2 and at constant agitation (±100 rpm). The plate was pre-coated with 500 µL of 2.5% poly(2-hydroxyethyl methacrylate) (p-HEMA) solution (Sigma-Aldrich), and dried for 48 h in a sterile culture cabinet prior to cell plating, in order to eliminate hepatocyte attachment, as described previously (Baron *et al.*, 2017; Hultman *et al.*, 2019; Lammel *et al.*, 2019).

In all cases, medium replacement was carefully performed on alternate days, with removal of 1.5 mL of old media and addition of 1.5 mL of fresh one. Collection of spheroids was performed on the 4th 8th, 11th, 14th, 18th, 22nd, 28th and 30th days post-isolation, for determination of cellular viability, biometrical measurement and morphological evaluation.

The most appropriate growth medium and time-points were selected, and optimization assays were carried out in 6-well microplates with 3 mL of DMEM/F-12 with 15 mM HEPES, 10 mL/L of antibiotic/antimycotic solution and charcoal FBS 10% (v/v), at a density of 0.5×10^6 cells/mL, at 18 ºC, without additional supply of O_2/CO_2 and constant agitation (±100 rpm). Media replacement was performed on alternate days as described. Sampling of the spheroids was performed on the 4th, 8th, 14th, 18th, 22nd and 28th days post-isolation and processed according to each specific endpoint (viability assessment, biometry evaluation, immunohistochemistry and light microscopy.

For test condition II n = ≥ 25 spheroids/day were used for biometric measurements (whenever it was possible), from each of the three fish (a total of 90 spheroids). Whereas for test conditions I and III n = ≥ 25 spheroids/day (if possible) from one fish were used. Test condition IV was discarded since it was not possible to perform any of the assays.

2.4.2 Design of 3D 5α-DHT Exposure Assays

Following hepatocyte isolation, for 5α-DHT exposure assays, cellular suspensions were plated at a density of 0.5×10^6 cells/mL in 6-well plates, with 3 mL/ well of complete DMEM/F-12 medium with 10% FBS, 15 mM HEPES and 10 mL/L of antibiotic/antimycotic solution, incubated at 18 ºC without additional supply of O_2/CO_2 and at constant agitation (±100 rpm).

Brown trout's primary hepatocyte spheroids from 2 immature fish were exposed for 96 h to 2 concentrations of 5α-DHT, namely, 10 (DHT5) and 100 µM (DHT6). The assay also included a control - C (supplemented DMEM/F-12 medium) and a solvent control - SC (0.1% ethanol in complete DMEM/F-12 medium) groups.

The spheroids were exposed to 5α-DHT between the 14th and 18th day of their growth. Medium exchange was performed after 48 h (on the 16th day), by replacing the maximum volume possible, without aspiration of the spheroids (± 2.3 mL), of old solutions by fresh ones. A total of 2 plates were used for each fish. In every plate, a single well was assigned to each condition, resulting in a total of 4 wells/condition. After the exposure period, the spheroids were sampled for different purposes (viability assessment, immunohistochemistry, light microscopy, TEM and molecular analyses) and processed accordingly.

2.4.3 Biometric Parameters of Brown Trout Hepatocyte Spheroids

Hepatocyte spheroids were daily photographed under a 10x or 20x objective lens, using a DP21 digital camera coupled to an Olympus BX50 light microscope. For spheroids with bigger sizes an Olympus SZX10 stereo microscope was used. In optimization experiments, ≥ 25 photographs of distinct spheroids were taken from various wells on each sampling day (if possible). Regarding 5α-DHT exposures, a minimum of 15 photos were taken for each condition in test.

TIFF photos were formatted in "TIFF.tiff" with ImageJ software version 1.52a (https://imagej.nih.gov/ij/), in order to be inputted in the AnaSP software program (https://sourceforge.net/projects/anasp/), specific for the quantitative assessment of multicellular spheroids' morphological parameters (Piccinini, 2015).

For the morphometric analysis of the spheroids with AnaSP, a photo was initially selected, and the limits of a specific spheroid were manually designed ("perform manual

segmentation only"). This process generates a binary mask of the spheroid's shape. For parameter calculation, data extraction was performed by inputting the binary mask on the software. The used outputs were equivalent diameter, area, volume and sphericity. The equivalent diameter corresponds to the diameter of the equivalent circle with the same area as the spheroid in analysis, as described by the developer of the software (Piccinini, 2015). For the parameters in which the result unit is displayed by default in pixels, a conversion was made to µm, by inputting in ImageJ the corresponding photo scale bar.

2.4.4   Viability Assays

Two assays were performed to evaluate the viability of 3D spheroids, specifically, 3-(4,5-dimethylthiazol-2-yl)-2,5-diphenyltetrazolium   bromide   (MTT)   and   resazurin reduction assays.

MTT reduction assay allows the quantification of a purple formazan product by measuring the optical density at 570 nm. This product results from the cleavage of MTT by enzymes in active mitochondria, therefore reflecting the amount of viable cells (Hussain *et al.*, 1993; Riss *et al.*, 2013). MTT colorimetric assay was first described by Mosmann (Mosmann, 1983) and has been subsequently optimized (Denizot & Lang, 1986; Hussain *et al.*, 1993). Ho *et al.* (Ho *et al.*, 2012) performed slight modifications to the original protocol for cytotoxicity assessment on multicellular tumour spheroids and, herein, the latter method was adapted for evaluation of cellular viability on spheroids from brown trout primary hepatocytes.

The spheroids were transferred from 6-well microplates to flat-bottom 96-well microplates (Orange Scientific), with one spheroid per well, and 100 µL of culture medium. A stock solution of 5 mg/mL of MTT (Sigma-Aldrich) was prepared in sterilized PBS (1x), and 10 µL were then added to each well (final concentration of 0.45 mg/mL/well). Plates were covered in foil and incubated at 18 ºC for 3 h. Plates were centrifuged at 1000g for 5 min in a ROTINA 380 R centrifuge (Hettich), with a plate rotor (380RPLATE Package). Then, the maximum supernatant was removed without suction of the spheroids, and formazan precipitates were dissolved in 50 µL of dimethyl sulfoxide - DMSO (Sigma-Aldrich), by shaking the plates in a Multi shaker FMS3 (FinePCR) for 1h. Absorbances were read at 570 nm and 620 nm (as reference wavelength) with a Multiskan GO (ThermoFisher). Three blank wells were performed by adding the same amount of medium, MTT and DMSO in the wells without cells.

Regarding culture optimization assays, a minimum of 4 spheroids from different wells were collected for MTT assay. In this case, absorbances of the spheroids from each sampling day were plotted over time.

Considering the 4 plates from the exposure assay, a minimum of 3 spheroids were collected from each exposed well in each plate, resulting in at least 6 spheroids/ condition for each fish. For viability assessment, absorbance values at 620 nm reference wavelength were subtracted from the values at 570 nm, in order to adjust for the optical variation of the wells, as well as, correction for possible dirt. Following adjustments, semi quantification of cellular metabolic activity was achieved by comparison of the values from exposed wells with values from control wells (Riss *et al.*, 2013), as follows:

$$\%Viability = \frac{Absorbance\ Exposed\ well}{Absorbance\ Control\ well} \times 100$$

The second viability test performed was the resazurin reduction assay. Viable cells have the ability to reduce the dye used in this assay into a pink fluorescent product, resorufin. The level of reduction is proportional to the number of living cells. Quantification is achieved by generating both resazurin and relative fluorescent units (RFU) at 530 nm and 590 nm (Ivanov *et al.*, 2017; Riss *et al.*, 2013).

Spheroids were transferred from 6-well microplates to flat-bottom 96-well microplates, and 198 µL of culture medium were added into each well (with a single spheroid). A stock solution of 1 mM of resazurin (Cayman Chemical Company) was prepared in sterilized PBS (1x) and stored at room temperature protected from light. In each well, 2 µL of stock solution were added, resulting in a final concentration of 10 µM of resazurin/well. The plates were wrapped in foil, and incubated at 18 ºC for 3 h, at constant agitation (±100 rpm). Fluorescence was read at 530 nm and 590 nm excitation and emission wavelengths respectively, with a Synergy™ HTX Multi-Mode Microplate Reader, using Gen5 software (Biotek, Agilent). Three wells with resazurin dye and without cells were performed. The procedures described here were based on protocols specifically adapted for 3D cultures (Eilenberger *et al.*, 2018; Ivanov *et al.*, 2017, 2014; Riss *et al.*, 2013; Walzl *et al.*, 2014).

For optimization experiments, minimum of 4 spheroids from different wells were collected for Resazurin assay. Again, absorbances of the spheroids from each sampling day were plotted over time.

Concerning the 3D spheroid 5α-DHT exposure assay, a minimum of 3 spheroids were collected on the 18th day from each of the exposed wells, resulting in at least 6 spheroids/condition for each fish for resazurin assay. Fluorescence values for each

sample were adjusted by background subtraction, that is, subtraction of the blank wells without cells from all values. Then, viabilities were calculated by applying the formula (Eilenberger *et al.*, 2018):

$$\%Viability = \frac{RFU\ Exposed\ well}{RFU\ Control\ well} \times 100$$

2.4.5 Light Microscopy - Qualitative Analysis

Individual spheroids (1 spheroid/well) were fixed in 200 μL of 3.7 - 4.0% w/v formaldehyde buffered to pH=7 and stabilized with methanol (PanReac AppliChem) in 96-well plates for 24 h, at room temperature and changed to ethanol 70% for another 24 h. The samples were then transferred to 1.5 mL eppendorf tubes (Merck), covered with Richard-Allan Scientific HistoGel (Thermo Scientific), and inserted into embedding cassettes after solidification, followed by incubation in ethanol 70%, until further processing.

Spheroids were submitted to a 12 h routine histological procedure in an automatic processor (Leica TP 1020), following the next steps: ethanol 70% (1 h), ethanol 90% (1 h), ethanol 96% (1 h), ethanol 99.9% (1 h), ethanol 99.9%/xylene (1 h), xylene (1 h), xylene/paraffin (1 h) and paraffin (2 h).

After processing, spheroids were embedded (Leica EG 1140 C) in paraffin (Thermo Scientific Histoplast), and the obtained blocks were sectioned at 3 μm in a fully automated rotatory microtome (RM2255 Leica Biosystems). A minimum of 2 sections/slide for staining protocols and a minimum of 3 sections/slide for immunohistochemistry protocols were acquired. After drying (1 h at 60 ℃, or at least 24 h at 37 ℃), the slides were stored at -20 ℃ until further use.

Detailed staining protocols are presented in Appendix C- Appendix EHematoxylin & Eosin (H&E) was used for general tissue structure assessment, Periodic Acid Schiff (PAS) followed by PAS with diastase allowed the identification of glycogen, and Masson's Trichrome differentiated between collagen fibres and muscular fibres. All sections were qualitatively observed under an Olympus BX50 light microscope, and photographs were taken using a DP21 digital camera.

For the optimization assays, a minimum of 4 spheroids from different wells of each 6-well microplate were collected for light microscopy at each time-point. While on the spheroid exposure assays, 2 spheroids were collected from each exposed well, whenever it was possible.

2.4.6   **Immunohistochemistry**

Sections were initially deparaffinized in xylene (2x 10 min), rehydrated through graded ethanol and washed in tap water. Antigen retrieval method was distinct according with the antibody. For caspase-3, the slides were heated in citrate buffer 0.01 M pH 6 in the pressure cooker, until reaching maximum pressure, after which 3 min. were counted. For E-cadherin, the slides were immersed in EDTA buffer at pH 9 with 0.05% TWEEN 20 (Sigma-Aldrich) and pre-heated in the microwave at 600W, until reaching the boiling point, from which 10 min were counted. From this point, the steps were equal for both antibodies.

After cooling of the slides to room temperature, a wash in distilled water was performed. Endogenous peroxidase was blocked with 3% hydrogen peroxide (Merck) in methanol (Honeywell) for 10 min. This step is essential for preventing non-specific background staining. Two 5 min washes in Tris buffered saline (TBS) buffer were performed before protein block with Novolink™ Max polymer Kit (Leica Biosystems, Germany). The optimal primary antibody dilutions were the following: polyclonal Rabbit Anti-Caspase-3 antibody (ab13847 abcam, UK) was diluted in PBS with 5% albumin bovine serum (BSA , NZYTech) for an optimized final dilution of 1:5000; monoclonal Mouse Anti-Human E-cadherin (M3612 Dako, Agilent) was diluted 1:50 in PBS with 5% BSA.

Sections were totally covered with the corresponding diluted primary antibody and incubated overnight using a humidified chamber. Negative sections were incubated with PBS with BSA 5%. Subsequent to incubation, the slides were washed 2x for 5 min in TBS with 0.05% TWEEN 20. Incubation of the slides in post primary was then performed for 30 min, consisting on a Rabbit anti mouse immunoglobulin G (IgG) from the Novolink™ Kit, followed by 2x 5 min washes in TBS with 0.05% TWEEN 20. The sections were incubated in Novolink™ Polymer for 30 min. Again, the slides were washed 2x with TBS with 0.05% TWEEN 20 for 5 min. A 3,3'-diaminobenzidine (DAB) working solution was prepared with DAB chromogen and DAB Substrate Buffer from the Novolink kit, for a final dilution of 1:20 providing the manufacturer's instructions. This substrate/chromogen solution ensures peroxidase development within 2-3 min of incubation. The slides were washed in distilled water and counterstaining was achieved with Mayer's Hematoxylin (Merck) for 1 min, followed by a 5 min rinse in tap water. Next, slides were dehydrated, cleared with xylene and mounted with Q Path® Coverquick 2000 media (VWR). Sections were photographed with a DP21 digital camera coupled to an Olympus BX50 light microscope.

2.4.7   Transmission Electron Microscopy

For primary fixation of spheroids, 150 μL of 2.5% glutaraldehyde in cacodylate buffer 0.1 M (pH 7.2, fresh) were added to the wells of a 96-well microplate (1 spheroid/well) and incubated for 2 h at 4 °C. The maximum volume was removed without aspiration of the spheroids, and then 2 washes in cacodylate buffer 0.1M were performed for 10 min at 4°C. Again, the maximum volume was removed from the wells and the post-fixation step consisted in adding 100 μL of 1% osmium tetroxide (fresh, prepared from 4% OSO_4 in cacodylate buffer 0.1 M) for 2 h at 4 °C. A subsequent wash in cacodylate buffer 0.1 M, pH 7.2 was performed for 10 min, after which the spheroids were transferred to 1.5 mL ppendorf tubes and totally covered in specimen processing Richard-Allan Scientific™ HistoGel™ (Thermo Scientific). The samples were place at 4 ºC for 20 min to allow solidification of the Histogel and incubated in 200 μL of cacodylate buffer 0.1 M at 4 ºC.

Dehydration of the tissues was achieved by several 30 min incubations of the samples in a graded series of ethanol with increasing concentrations, using a volume of 200 μL, as follows: 50 % ethanol, 70% ethanol, 90% ethanol, 95% ethanol, 100% ethanol I, 100% ethanol II. Transition between ethanol and embedding resin was attained by incubating the samples twice for 15 min in propylene oxide (Merck).

For epoxy resin preparation equal volumes of Epon A and Epon B were mixed, and gently agitated for ±10 min. The proper amount of 2,4,6-tris (dimethylaminomethyl) phenol - DMP-30 (Difco) accelerator and curing agent was added to the mixture, and again agitated for at least 25 min. Epon A and B were obtained as follows:

Epon A – Glycindether 100 (31 mL, Merck) was mixed with the curing agent dodecenylsuccinic anhydride (50 mL, Difco) and stored at 4 ºC until further use.

Epon B – Glycindether 100 (50 mL) was mixed with the curing agent methyl nadic anhydride (44.5 mL, Fluka) and stored at 4 ºC until further use

The following mixtures were prepared previously to their use (to ensure proper homogenization), and ± 200 μL were added to each Eppendorf, as follows: propylene oxide + Epon 3:1 mixture for 1h; propylene oxide + Epon 1:1 mixture over night at 4 ºC; propylene oxide + Epon 1:3 mixture for 1h (with freshly prepared Epon); Epon for 1h (freshly prepared); Epon for 10 min at 60 ºC. After incubations, Epon was inserted in the TEM moulds, and the spheroids were positioned in each edge of the blocks. The moulds were incubated at 60 ºC, and after 1 h the spheroids had to be readjusted to the edges of the moulds before total polymerisation at 60 ºC for 48 h.

Resin blocks were sectioned at 1.250 µm in an Ultramicrotome Leica EM UC7 (Leica Microsystems) to obtain semithin sections using adhesive slides, while ultrathin sections were obtained at 90 nm and collected using hexagonal 200 mesh copper 3.05mm grids (Agar Scientific).

For semithin staining the sections were incubated in 1% methylene blue (Merck) for ±45 sec, washed in distilled water and dried. Ultrathin grids were contrasted by immersion in uranyl acetate (Merck) and incubated for 20 min in the dark. The grids were rinsed in distilled water for two sets of 1 min and dried in filter paper, followed by immersion in drops of lead citrate (Merck) for 10 min. Again, the grids were rinsed vertically in distilled water for two sets of 1 min and dried in filter paper. Grids were observed under a JEOL 100CXII transmission electron microscope (JEOL, Tokyo, Japan) operated at 60 kV, and photos were acquired through a SC1000 CCD digital camera (Gatan, Pleasanton).

In the 3D culture optimization experiment, for each time-point a minimum of 4 spheroids from different wells of the 6-well microplates were collected for TEM. If possible, 2 spheroids from each condition were collected for ultrastructural analysis of spheroids from 5α-DHT exposures.

2.4.8   RNA Extraction, cDNA Synthesis and RT-qPCR

In the 5α-DHT exposure experiments, a minimum of 42 and a maximum of 160 spheroids were collected in duplicate/well from each fish, if possible. Brown trout primary hepatocyte spheroids' total RNA extraction, cDNA synthesis and RT-qPCR were performed according to the protocol described in the sections 2.3.1 and 2.3.2.

2.5 Statistical Analyses

Analysis were performed using Past 3 software, version 3.24 (https://folk.uio.no/ohammer/past/), and graphs generated with GraphPad Prism 6 (https://www.graphpad.com/). Overall, statistical analyses were similar among results, namely, for molecular analyses of 2D and 3D experiments, for evaluation of biometric parameters from spheroids and, viability assessment for both 3D optimization and 3D 5α-DHT exposure experiments. One-way analysis of variance (ANOVA) was preceded by testing the assumptions of normality and homogeneity of data sets, using the Shapiro-Wilk W and Levene's tests, respectively. ANOVA analyses were performed, followed by evaluation of Tuckey's pairwise comparisons. For data that did not fulfil the parametric

tests' assumptions, the significance of the differences between pairs was studied by Mann-Withney test. Sequential Bonferroni corrections were applied to the latter, for adjustment of p values and reduction of false positives. Significance level was set at 95%, with significant differences when p value < 0.05.

Chapter 3. Results

3.1 mRNA Expression Levels of Brown Trout Primary Hepatocytes Exposed to 5α-DHT in 2D Cultures

Relative mRNA levels of lipid metabolism-related genes in monolayer cultures of brown trout primary hepatocytes exposed for 96 h to six concentrations of 5α-DHT are represented in Fig. 1. The *Acox1-3I* and *PPARγ* mRNA levels were not significantly influenced by the exposure to any concentration of 5α-DHT. As to *ApoAI*, a down-regulation was found after exposure to the highest 5α-DHT dose (DHT6), in comparison to the control groups, although no significant differences were registered. Regarding the *Acsl1* expression levels, a significant increase was noted after exposures to DHT4, DHT5 and DHT6, over DHT1, DHT2 and control groups. A dose dependent pattern was clear, at least at the highest doses. The *Fabp1* mRNA levels showed a clear tendency to increase, especially at the highest dose of 5α-DHT. However, significant differences between DHT6 and the control groups have not been proven.
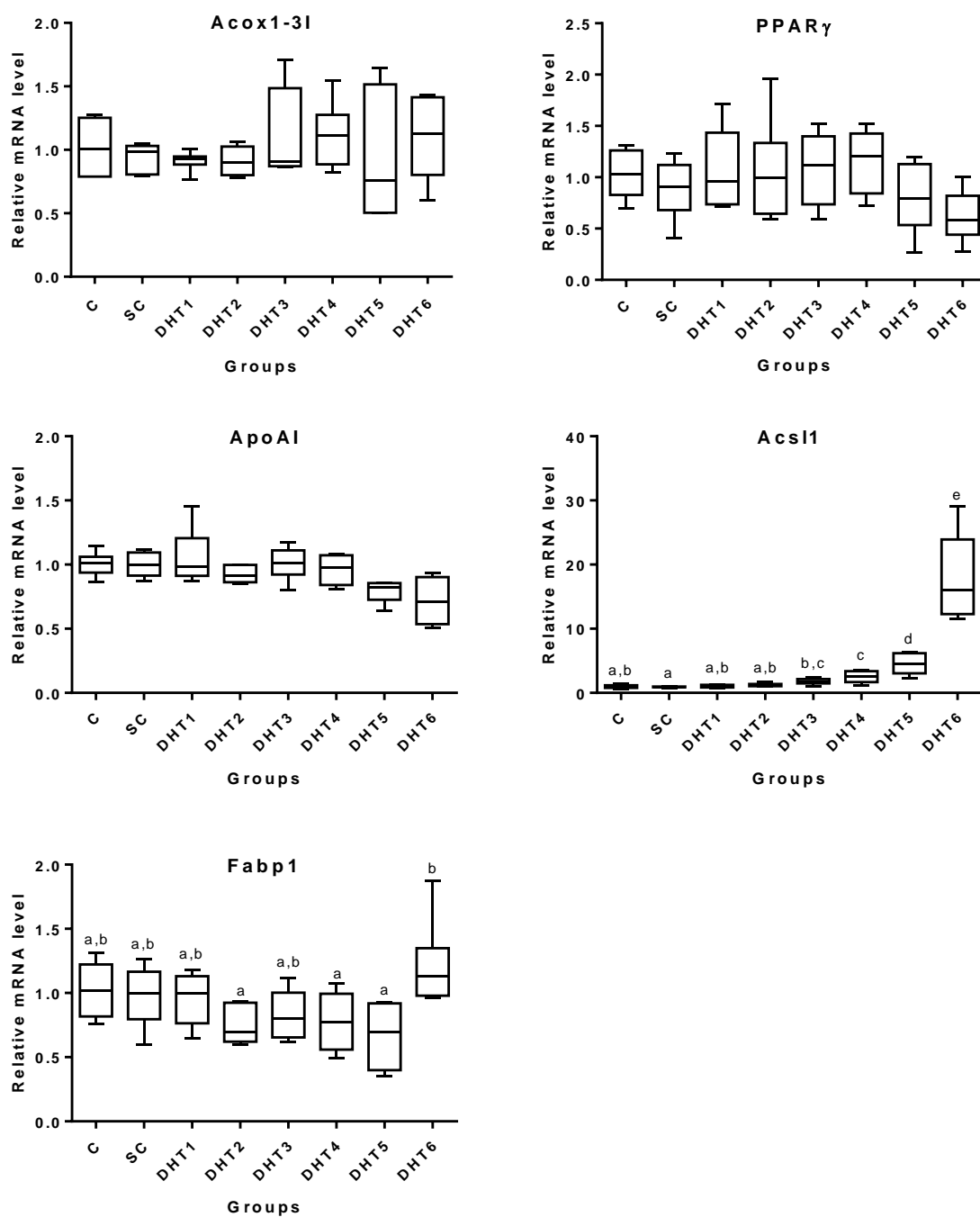
Fig. 1. Relative mRNA levels of lipid metabolism-related genes in brown trout primary hepatocytes after 96 h of exposure to: control – C (supplemented L-15 medium), solvent control – SC (0.1% ethanol in supplemented L15 medium), and six concentrations of 5α-dihydrotestosterone (DHT1 – 1nM, DHT2 – 10 nM, DHT3 – 100 nM, DHT4 – 1 µM, DHT5 – 10 µM and DHT6– 100 µM). Graphical data of *Acox1-3I* (acyl-coenzyme A oxidase 1 – 3I isoform), *PPARγ* (peroxisome proliferator-activated receptor gamma), *ApoAI* (apolipoprotein AI), *Acsl1* (acyl-CoA long chain synthetase 1) and *Fabp1* (fatty acid binding protein 1) mRNA levels are represented as median, minimum and maximum values. Significant differences between groups are shown by different letters according to Tuckey's pairwise parametric test or Mann-Withney with Bonferroni sequential corrections (for *Acox1-3I* and *ApoAI*).

3.2 Optimization of Culture Conditions for the Growth of 3D Spheroids from Brown Trout Primary Hepatocytes

In test condition IV (Leibovitz's L-15 medium without phenol red with antibiotic/antimycotic solution and FBS at 18 ºC and ±100 rpm, with 2.5% p-HEMA coating), after 24 h of culture, most of the hepatocytes formed large clusters, with a reduced number of dispersed isolated cells throughout the wells. No adherent cells were observed. By day three (72 h post-isolation), almost all cells were agglomerated in a single main aggregate of hepatocytes, with highly irregular shape and limits. This cluster persisted until the 30th day of culture. Results will be presented here for the remaining culture media tested (test conditions I, II and III).

3.2.1   Biometric Parameters

The biometric parameters of spheroids grown in test condition I (DMEM/F-12 with HEPES, antibiotic/antimycotic solution, and serum replacement 3 at 18 ºC and with ±100 rpm) are represented in Fig. 2. The equivalent diameter of spheroids increased significantly from the 4th to the 14th day post-isolation (Fig. 2A). Overall, diameter stabilization was reached on the 14th day in culture, with a median value of 339 µm. The highest median diameter of the spheroids was 772 µm on the 28th day. A similar pattern was observed for spheroids' area (Fig. 2B). A general stabilization of the area was noted from the 14th day in culture (with a median value of 2.03×10^5 µm^2). Regarding Fig. 2C, the sphericity remained nearly constant throughout the 30 days of culture, with a median value of 0.908. The volume of the spheroids displayed similar patterns as the equivalent diameter and area (Fig. 2D), stabilization occurred from the 14th with a median value of 2.14×10^8 voxels. Overall, spheroids grown in this medium were the largest among all tested conditions.
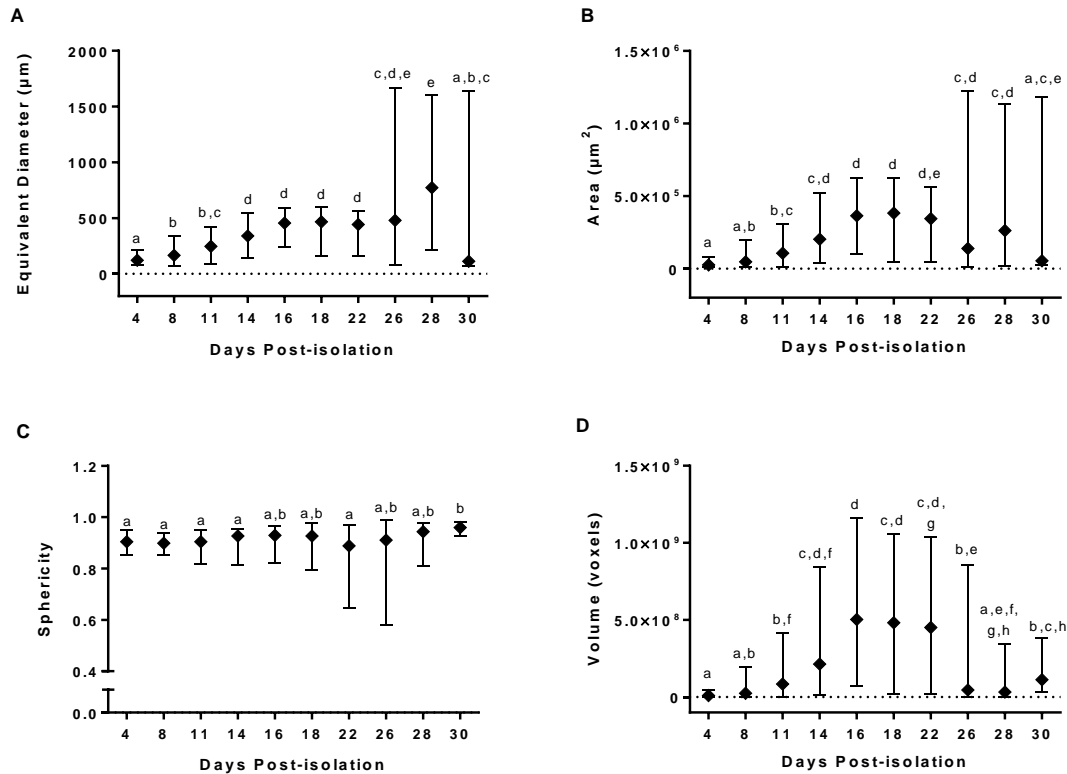
Fig. 2. Variation of the biometric parameters of spheroids cultured in DMEM/F-12 with 15 mM of HEPES, 10 mL/L of antibiotic/antimycotic solution and 20 mL/L of serum replacement 3 (test condition I), throughout the post-isolation days A. Equivalent diameter (μm) B. Area (μm^2) C. Sphericity and D. Volume (voxels). Values were generated by performing manual segmentation of each photograph (n = ≥ 25 spheroids) on the AnaSP software. Significant differences between days are shown by different letters according to Mann-Withney with Bonferroni sequential corrections.

In test condition II (DMEM/F-12 with 15 mM of HEPES, 10 mL/L of antibiotic/antimycotic solution and FBS 10% (v/v), at 18 °C and ±100 rpm), the median of the equivalent diameter of the spheroids significantly increased between the 4th and 16th days in culture (Fig. 3A). On the 8th day it had a value of 140 μm. From the 16th until the 28th day, equivalent diameters ranged from 58.8 to 536 μm (minimum to maximum), with a median value of 217 μm. The area revealed a similar variation as the equivalent diameter, with a significant increase in the values from the 4th until the 16th day (Fig. 3B). From the 16th until the 28th day, areas had no major significant variations, ranging from 6.08x10^3 to 5.07x10^5 μm^2 with a median of 8.25x10^4 μm^2. Regarding the sphericity, relatively constant values were observed along the 28 days in culture (Fig. 3C). From the 14th day post-isolation, median values remained consistent, without significant differences among days. The median of the sphericity from 14th to 28th day was 0.862, with a minimum of 0.611 and

a maximum of 0.977. The volume increased on the first days of the spheroids' growth, with the minimum reported on the 4th day (977280 voxels) (Fig. 3D). Stabilization occurred between the 14th/16th day until the 28th, with median volumes of 4.32×10^8 and 7.41×10^8 voxels, respectively.

Fig. 3. Variation of the biometric parameters for spheroids cultured in DMEM/F-12 with 15 mM of HEPES, 10 mL/L of antibiotic/antimycotic solution and FBS 10% (v/v) at 18 ºC and with ±100 rpm (test condition II), throughout the post-isolation days A. Equivalent diameter (µm) B. Area (µm^2) C. Sphericity and D. Volume (voxels). Values were generated by performing manual segmentation of each photograph (n = 90 spheroids, whenever possible) on the AnaSP software. Significant differences between days are shown by different letters according to Mann-Withney with Bonferroni sequential corrections.

For test condition III (Leibovitz's L-15 without phenol red, with 10 mL/L of antibiotic/antimycotic solution and FBS 10% (v/v) at 18 ºC and with ±100 rpm), the variation of the median values of the biometric parameters are presented in Fig. 4. The equivalent diameter remained relatively constant until the 26th day of culture. On the 28th and 30th days a significant increase was observed, in comparison to the first days of the spheroid's growth. Median values ranged from 38.5 to 375 µm (minimum to maximum) from the 4th until the 30th days post-isolation, with the median value being 99.7 µm. A

comparable constant pattern (1.59×10^4 µm^2 on the 14th day) was found for the area (Fig. 4B). A significant increase on the 28th and 30th days was noticed, with the maximum value reached on the latter day (2.48×10^5 µm^2). Sphericity from spheroids grown in these conditions displayed only minor variations over time (Fig. 4C), with a median of 0.927 from the 4th until the 30th day. Sphericity levels decreased on the 26th day, differing significantly from the 4th to 16th days of culture. The maximum value of 0.994 was reached on the 30th day. Finally, the medians of the spheroids' volume stabilized between the 14th – 30th day, with 5.54×10^6, 2.99×10^5 and 2.50×10^8 voxels as median, minimum and maximum, respectively (Fig. 4D). Again, on the 28th and 30th days of culture, a slight increase was noticed on the volumes. Overall, the spheroids cultured with this medium were the smallest among all tested conditions.
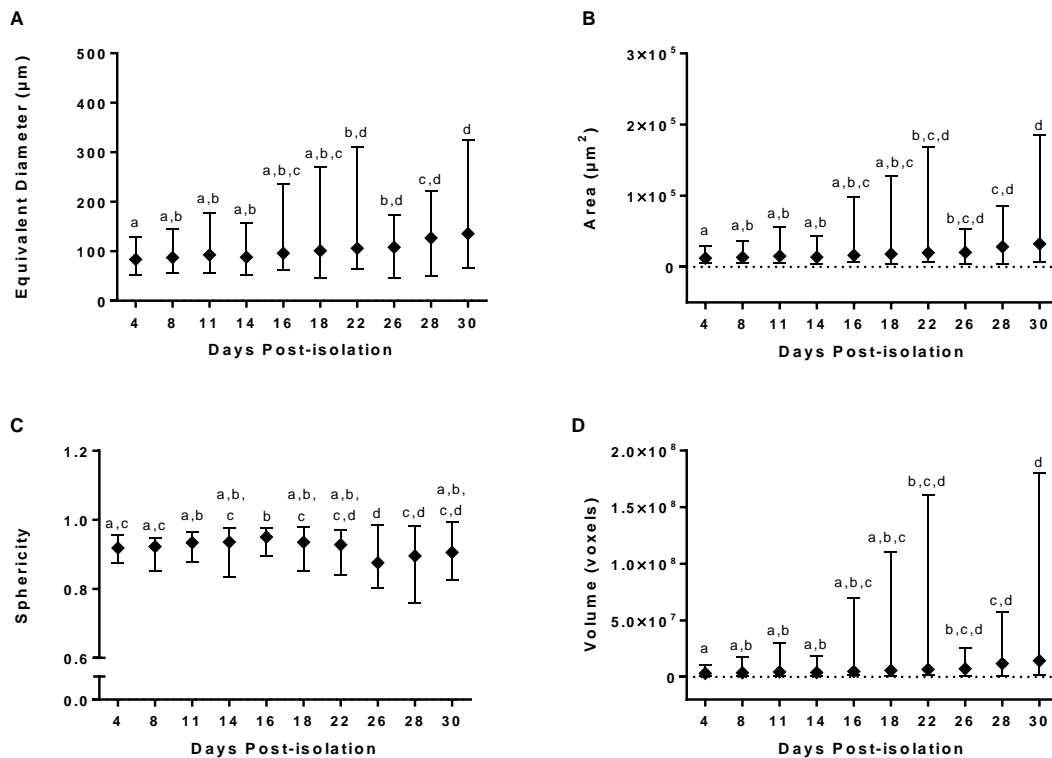
Fig. 4. Variation of the biometric parameters for the spheroids cultured in Leibovitz's L-15 without phenol red, with 10 mL/L of antibiotic/antimycotic solution and FBS 10% (v/v) at 18 °C and with ± 100rpm (test condition III), throughout the post-isolation days. A. Equivalent diameter (µm) B. Area (µm^2) C. Sphericity and D. Volume (voxels). Values were generated by performing manual segmentation of each photograph (n= ≥ 25 spheroids whenever possible) on the AnaSP software. Significant differences between days are shown by different letters according to Tuckey's pairwise parametric test or Mann-Withney with Bonferroni sequential corrections (for the sphericity).

3.2.2 Viability Assessment

For test conditions I and III, the MTT viability assay was performed (Fig. 5). In both cases, the variation of absorbances between days post-isolation was not statistically significant. However, for test condition I, an increase was observed on the 30th day, reaching the maximum value of 0.0828. As for test condition III, the median values of absorbances remained constant over time.
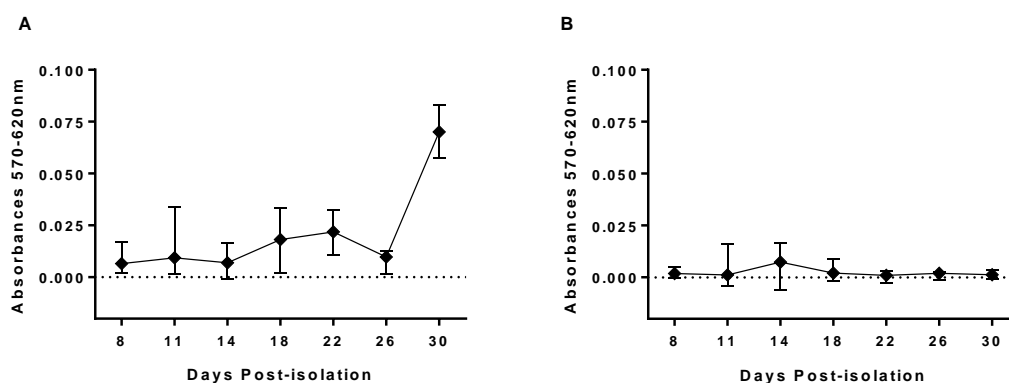
Fig. 5. MTT viability assay from spheroids cultured in: A. DMEM/F-12 with 15 mM of HEPES, 10 mL/L of antibiotic/antimycotic solution and 20 mL/L of serum replacement 3 (test condition I) and B. Leibovitz's L-15 without phenol red, with 10 mL/L of antibiotic/antimycotic solution and FBS 10% (v/v) (test condition III). Absorbance values (570 – 620 nm) were plotted against each day post-isolation. Statistical analysis was performed by Mann-Withney with Bonferroni sequential corrections.

The MTT and resazurin viability assays were performed for test condition II. Variation of Absorbance (A) and RFU (B) values of the spheroids were recorded for 28 days, according to each assay (Fig. 6). As reported by the MTT assay, median absorbance values of the spheroids increased from the 8th until the 22nd day (Fig. 6A). This variation is statistically significant between the 8th and 18th and between the 8th and 22nd days.

Concerning the resazurin assay in Fig. 6B, RFU values did not vary significantly until the 18th day (with a median of 31.8 RFU from the 8th until the 18th day). On the 22nd day post-isolation, a significant increase of the median RFU values was observed, with a maximum of 846 RFU, and a median of 307 RFU.
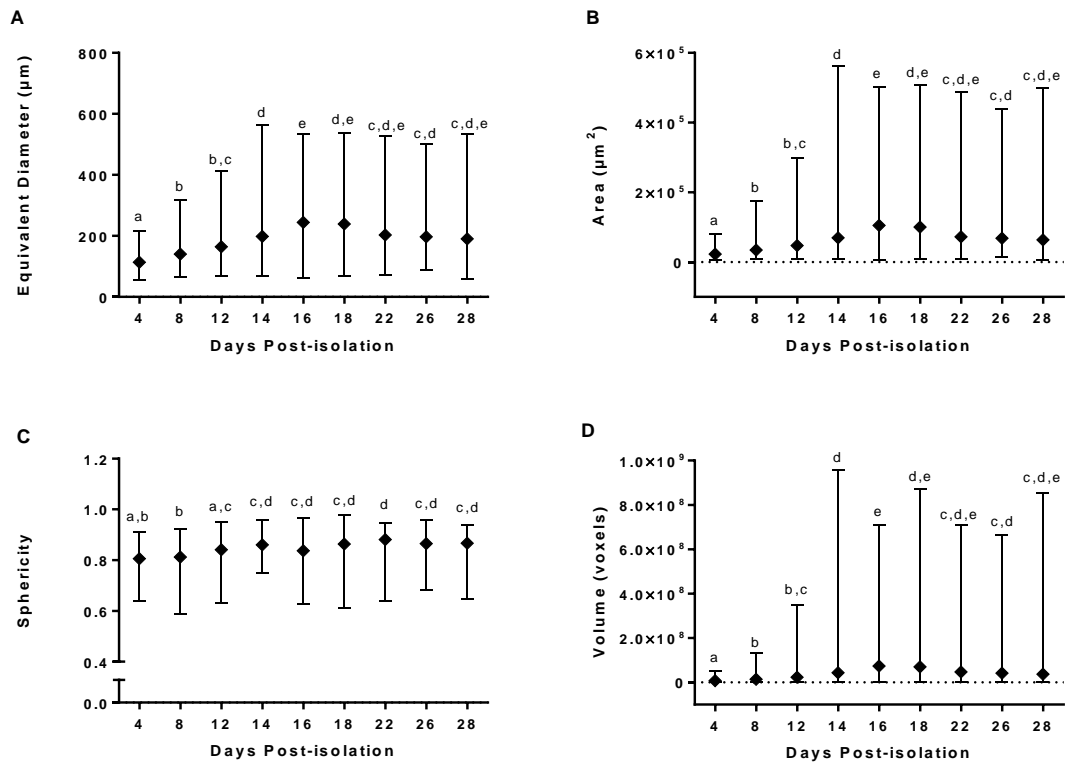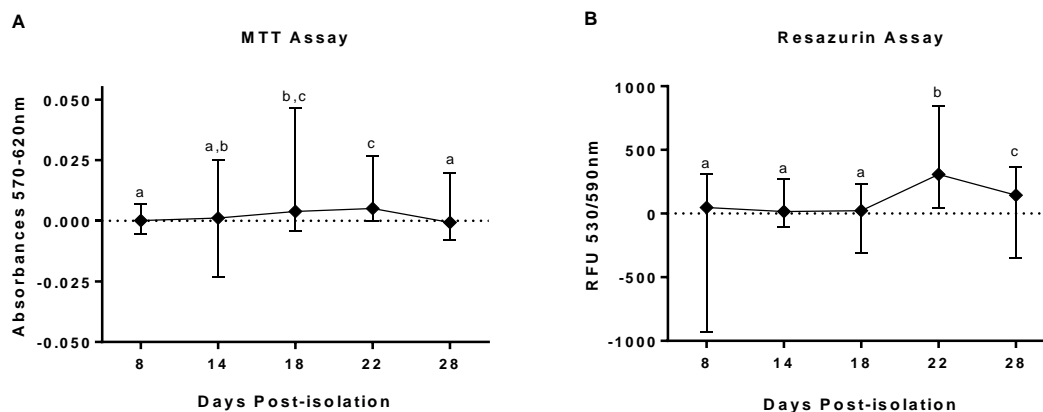
Fig. 6. Viability assays from spheroids cultured in DMEM/F-12 with 15 mM of HEPES, 10 mL/L of antibiotic/antimycotic solution and FBS 10% (v/v). A. MTT assay - Absorbance values (570 – 620 nm) were plotted against each day post-isolation. B. Resazurin assay - RFU values (530/590 nm) on each day post-isolation. Significant differences between days are shown by different letters, according to Mann-Withney with Bonferroni sequential corrections.

3.2.3 Morphology – Qualitative Analysis

In Fig. 7., the staining techniques used on paraffin sections of spheroids cultured in test condition I are exemplified. The spheroids from the 8th day are formed by compact hepatocytes (Fig. 7A). It is also possible to identify intact nuclei and cellular membranes (Fig. 7A and B). As spheroids achieved larger sizes over time, cells with strong eosin staining were observed in the centre of the spheroid (Fig. 7B). Vacuoles were present in all time points, but their quantity increased with the time in culture. PAS and PAS with diastase techniques allowed the identification of glycogen deposition (Fig. 7C and D), with lower intensities from the 22nd day onwards. The distribution of collagen fibres was relatively homogeneous throughout the spheroid from the 8th day (Fig. 7E). At longer culture times the blue trichrome staining predominated at the periphery of the spheroid (Fig. 7F).
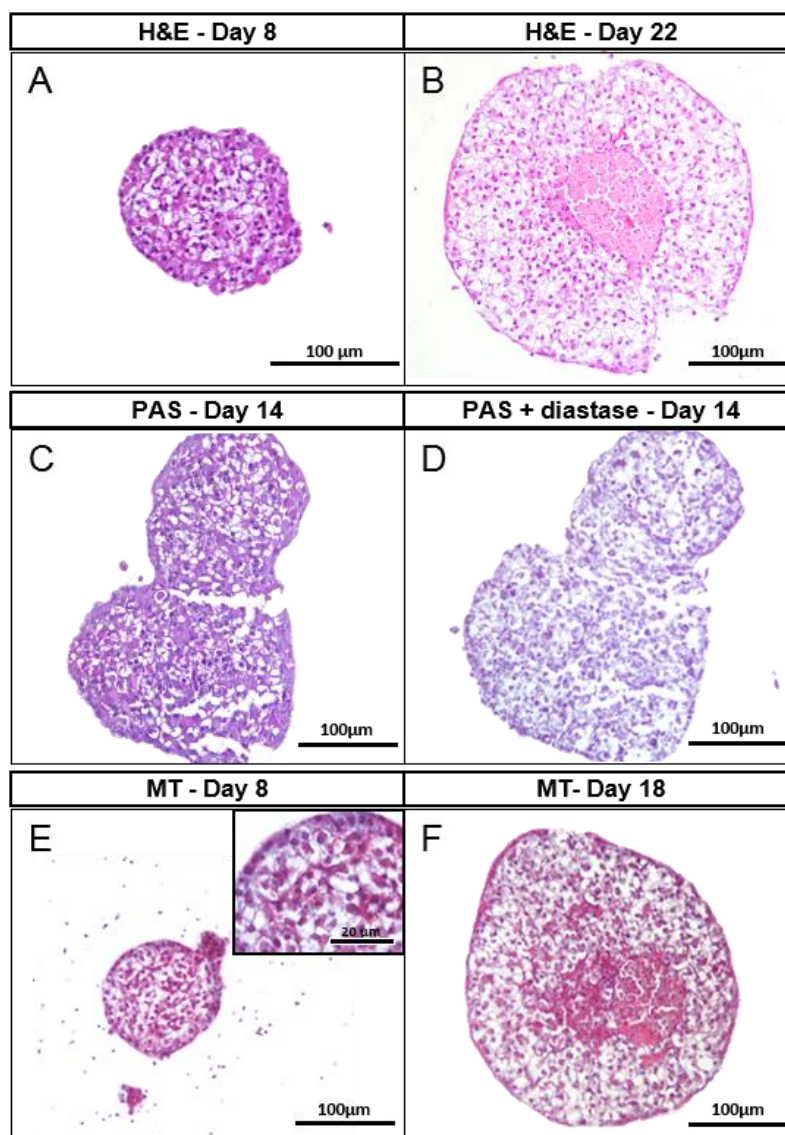
Fig. 7. Histological sections from brown trout spheroids cultured in test condition I (DMEM/F-12 with HEPES, antibiotic/antimycotic solution, and serum replacement 3 at 18 °C and with ±100 rpm). Paraffin sections were stained with H&E (A and B), PAS (C), PAS with diastase (D) and MT (E and F).

Considering test condition II, histological sections of spheroids are represented in Fig. 8. H&E staining demonstrates the development of spheroids over time, from Fig. 8A to E. Primary hepatocyte spheroids are compact with intact nuclei and highly spherical shapes in all time-points. Hepatocytes at the periphery of the spheroid displayed well-defined cellular membranes from the 14th day (Fig. 8B – E). Vacuoles are present in the spheroids from all time-points. PAS and PAS with diastase techniques (Fig. 8F – I) showed a disperse localization of glycogen in spheroids, with no major changes in staining intensities from the 8th (Fig. 8F and G) to 18th day (Fig. 8H and I). Regarding the identification of collagen fibres, MT showed intense blue staining in the intercellular

spaces across the 14 day-old spheroid (Fig. 8K). Blue stain intensity increased between day 8 (Fig. 8J) and day 22 (Fig. 8L), the latter predominating at the periphery of the spheroids.
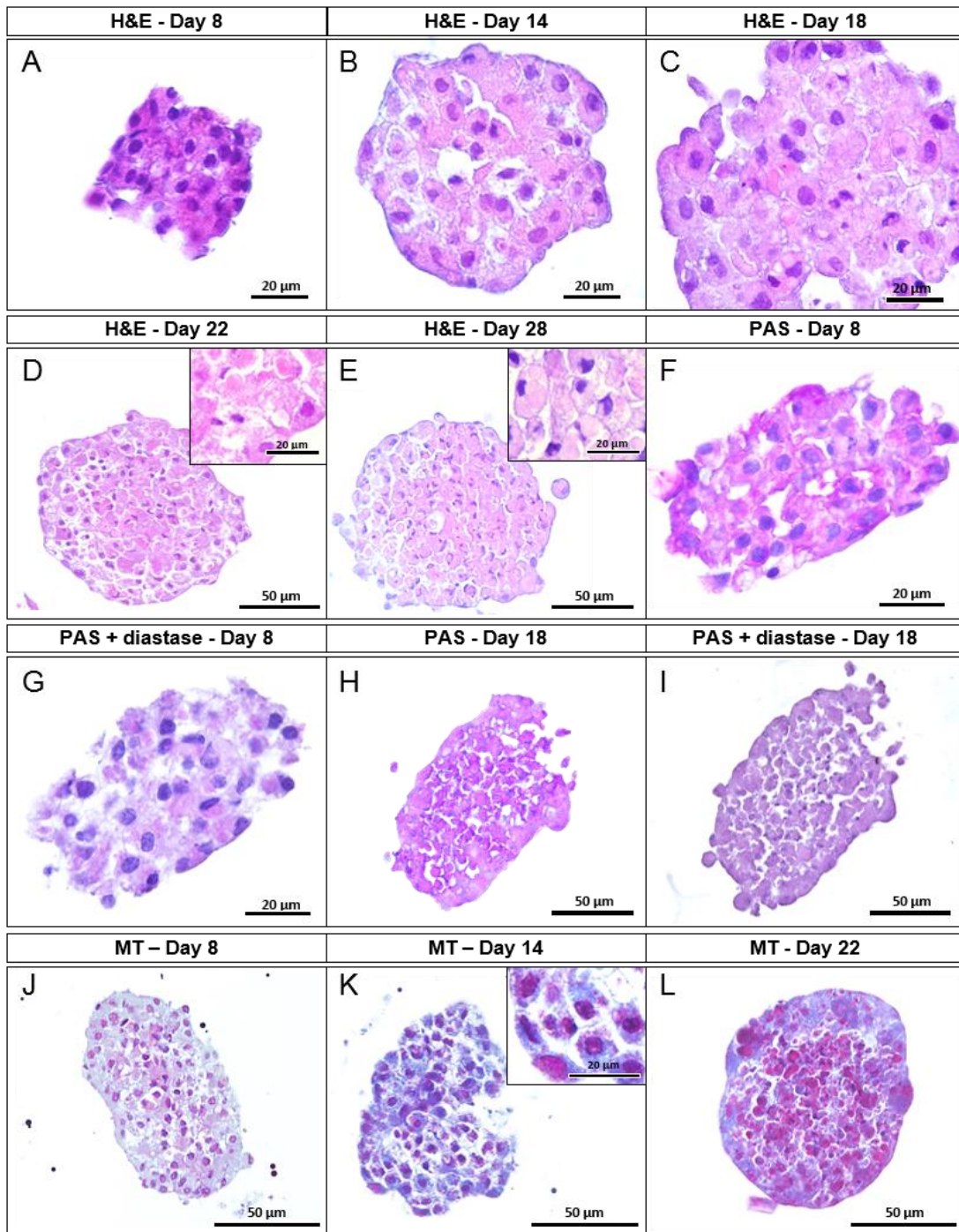
Fig. 8. Histological sections from brown trout spheroids cultured in test condition II (DMEM/F-12 with 15 mM of HEPES, 10 mL/L of antibiotic/antimycotic solution and FBS 10% (v/v), at 18 ºC and ±100 rpm). Paraffin sections were stained with H&E (A-E): PAS (F and H), PAS with diastase (G and I) and: MT (J-L).

Paraffin sections from spheroids grown in test condition III are shown in Fig. 9. Spheroids demonstrated intact nuclei and cellular membranes, with a highly spherical and compact structure over time (Fig. 9A. and B). In general, spheroids had a low number of cells, and therefore, display small sizes. Vacuoles were found in all time-points. In the 14th day (Fig. 9C and D), it is possible to identify deposition of glycogen distributed through the spheroid, according to PAS and PAS with diastase, respectively. Intensity of the staining decreases along with spheroid growth. Regarding MT, in Fig. 9E and F, collagen staining was present in spheroids from all the growth days, despite exhibiting very light intensities comparing with the remaining test conditions.
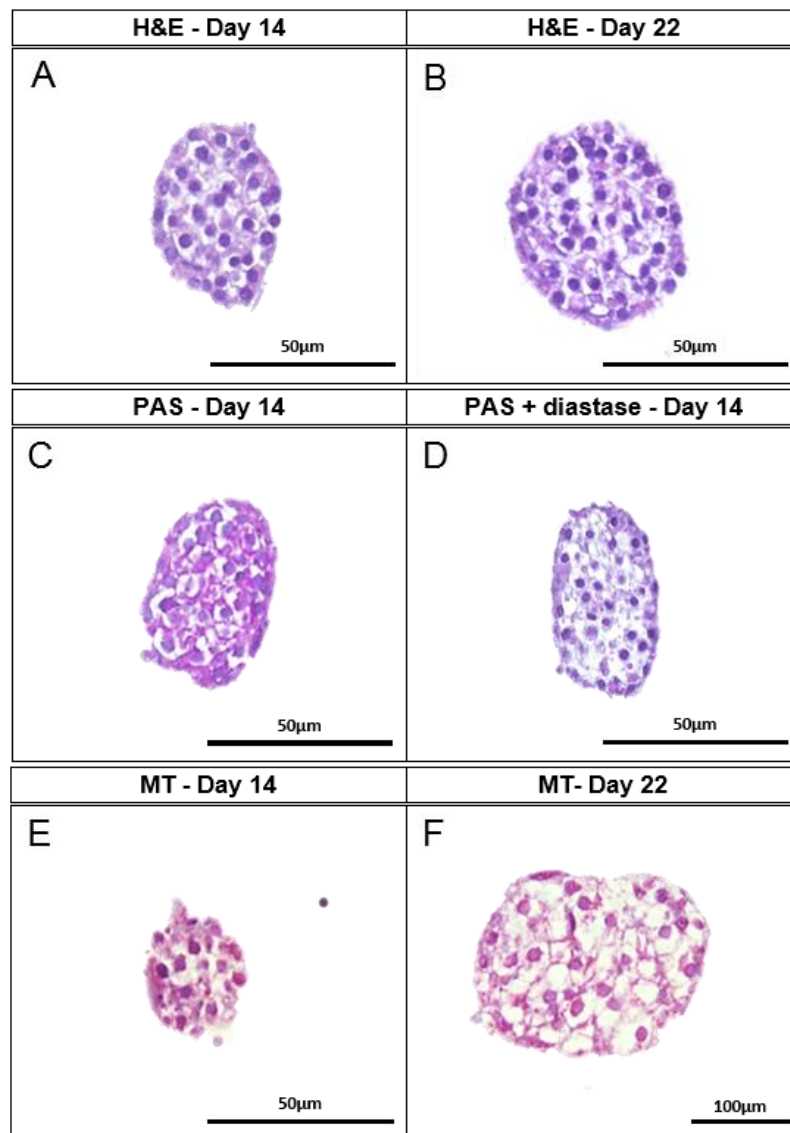
Fig. 9. Histological sections from brown trout spheroids cultured in test condition III (Leibovitz's L-15 without phenol red, with 10 mL/L of antibiotic/antimycotic solution and FBS 10% (v/v) at 18 ºC and with ±100 rpm). Paraffin sections were stained with H&E (A and B), PAS (C), PAS with diastase (D) and MT (E and F).

3.2.4 **Immunohistochemistry**

Immunohistochemistry with caspase-3 and E-cadherin are illustrated in Fig. 10. No immunostaining was observed in any of the negative controls.

Regarding test condition I, caspase-3 showed an intense marking of hepatocytes located in the centre of 18th day-old spheroids (Fig. 10A). Few and punctual cells are also stained throughout the spheroid. The apoptotic cells in the core are surrounded by non-apoptotic cells, creating a boundary of unlabelled cells around this centre. In Fig. 10B, it is clear that the distribution of E-cadherin across the spheroid is mainly located between cells.

For test condition II, immunohistochemistry for caspase-3 demonstrated punctual apoptotic cells with a homogeneous distribution throughout the spheroid, for both 14th and 18th days (Fig. 10C and D, respectively). Regarding E-cadherin immunohistochemistry (Fig. 10E and F), the intercellular spaces revealed an intense marking throughout the spheroid. The intensity and distribution of E-cadherin in spheroids did not varied among days in culture. Immunohistochemistry for caspase-3 in test condition III showed few and dispersed apoptotic cells in the spheroids (Fig. 10G). For E-cadherin, an intense labelling of the intercellular spaces was observed. Distribution and intensity of the antibody's presence is comparable among days (Fig. 10H).
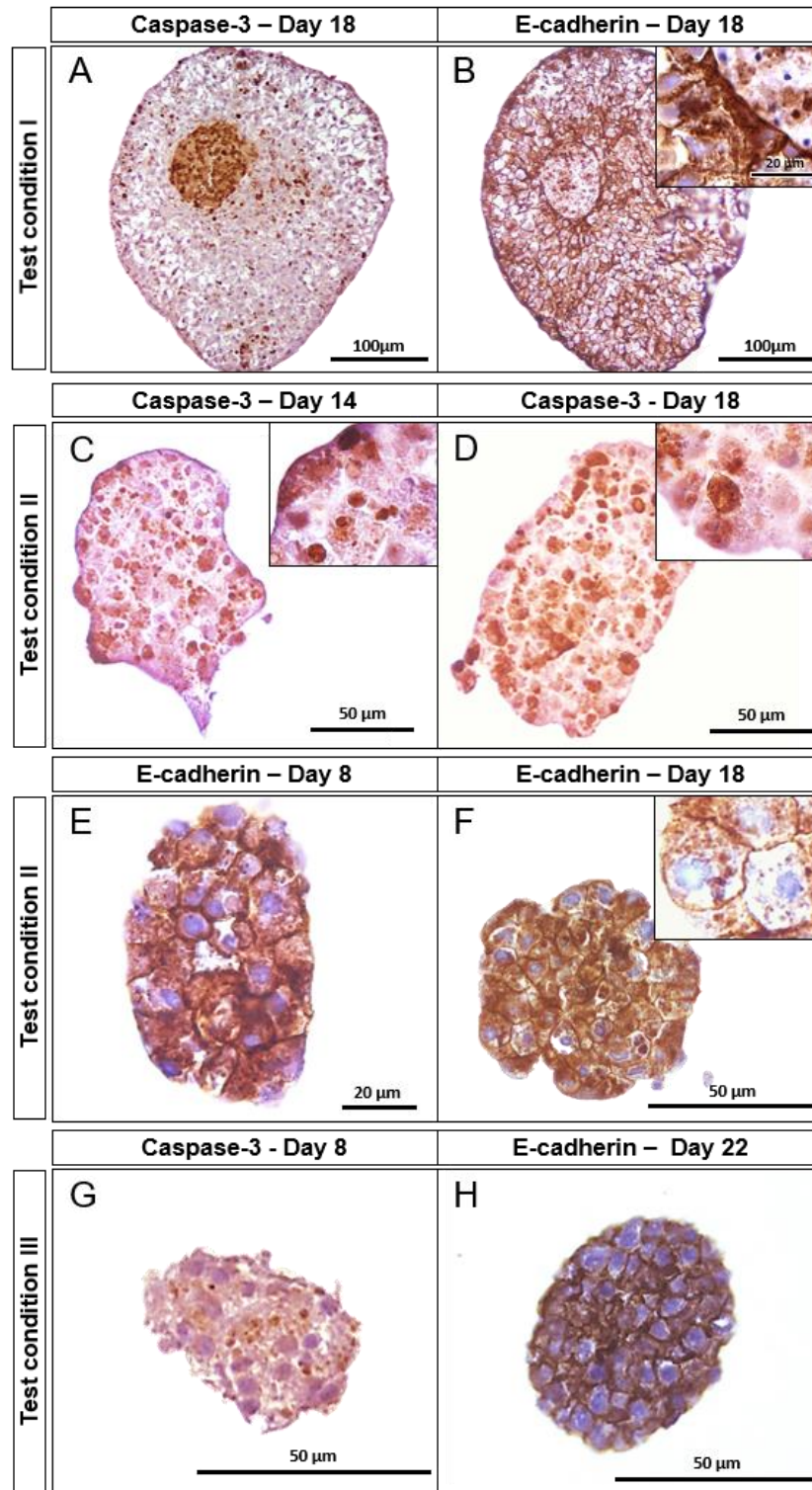
Fig. 10. Immunohistochemistry for caspase 3 (A, C, D and G) and E-cadherin (B, E , F and H) in brown trout spheroids cultured in different test conditions: I (DMEM/F-12 with HEPES, antibiotic/antimycotic solution, and serum replacement 3 at 18 ºC and with ±100 rpm), II (DMEM/F-12 with 15 mM of HEPES, 10 mL/L of antibiotic/antimycotic solution and FBS 10% (v/v), at 18 ºC and ±100 rpm) and III (Leibovitz's L-15 without phenol red, with 10 mL/L of antibiotic/antimycotic solution and FBS 10% (v/v) at 18 ºC and with ±100 rpm).

3.3 Exposure of 3D Spheroids from Brown Trout Primary Hepatocyte to 5α-DHT

3.3.1   Biometric Parameters

Exposure of 3D brown trout hepatocytes to 5α-DHT demonstrated no influence on the equivalent diameter of the spheroids (**Fig. 11**A). In fact, the median values for each group did not vary significantly. Similarly, the area of the spheroids was not significantly altered by any of the conditions tested (**Fig. 11**B). The minimum value for the area, 7920.18 µm^2, was found at DHT6 exposure dose. Also, the highest 5α-DHT concentration (DHT6) significantly decreased the sphericity of the spheroids, in comparison to the other groups (**Fig. 11**C). Sphericity values ranged from 0.633 to 0.854, with a median of 0.748 in the DHT6 condition. The highest median was reached at the C group with a sphericity of 0.860). As to the volume of the spheroids, medians revealed a stable pattern, with no significant differences between groups (**Fig. 11**D).
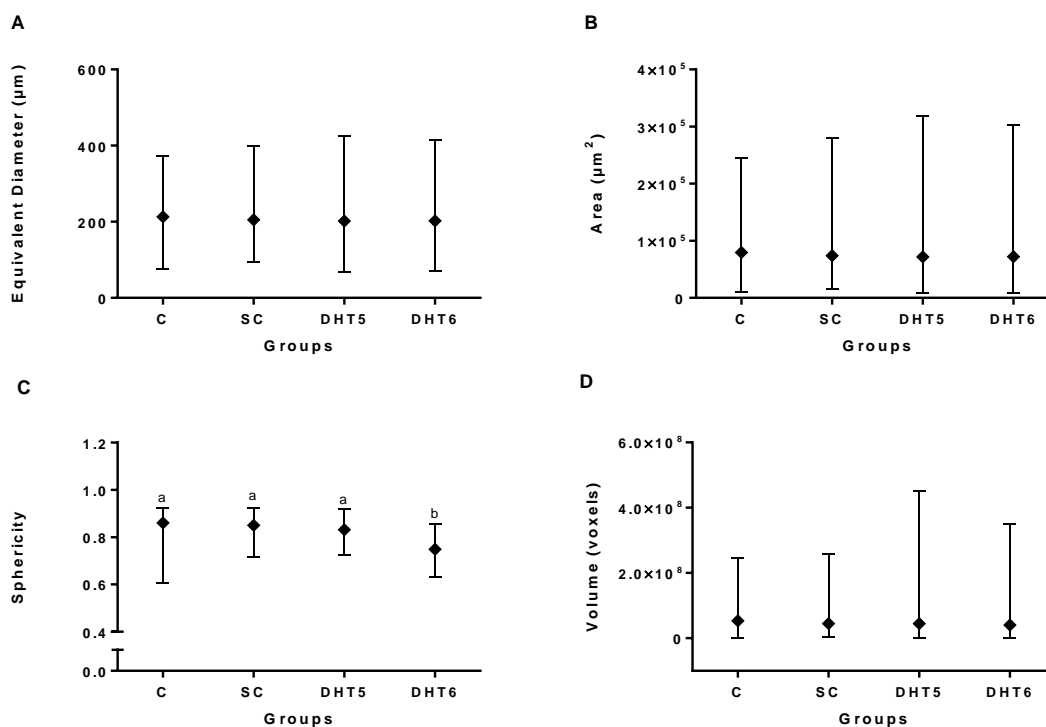
Fig. 11. Variation of the biometric parameters of 18-day-old spheroids after 96 h exposures to: control – C (supplemented DMEM/F-12 medium), solvent control – SC (0.1% ethanol in complete DMEM/F-12 medium), 10 µM of 5α-DHT – DHT5 and 100 µM of 5α-DHT – DHT6. A. Equivalent diameter (µm) B. Area (µm^2) C. Sphericity and D. Volume (voxels). Values were generated by performing manual segmentation of each photograph (minimum n = 46 spheroids, maximum n = 108 spheroids) on the AnaSP software. Significant differences between groups are represented by different letters, according to Mann-Withney with Bonferroni sequential corrections or Tuckey's pairwise parametric test (for the equivalent diameter).

3.3.2 Viability Assessment

Viability percentages according to the MTT and resazurin assays performed for hepatocyte spheroids exposed to 5α-DHT are shown in Fig. 12. For both assays, viability of the spheroids did not differ significantly between treatments.

For the MTT Assay, median values of the viabilities decreased in a dose dependent manner, however, significant differences were not confirmed according to the non-parametric analysis of the data (Fig. 12A). The maximum median achieved was 70.6 % for the C group and the minimum was 21.7 % for DHT6.

For the resazurin assay, an irregular pattern was noticed (Fig. 12B). An increase in the viabilities was observed for DHT5 condition, with the highest median registered (115.20 %). A decline in the viability of DHT6 group, with a median of 21.58 %, was found.
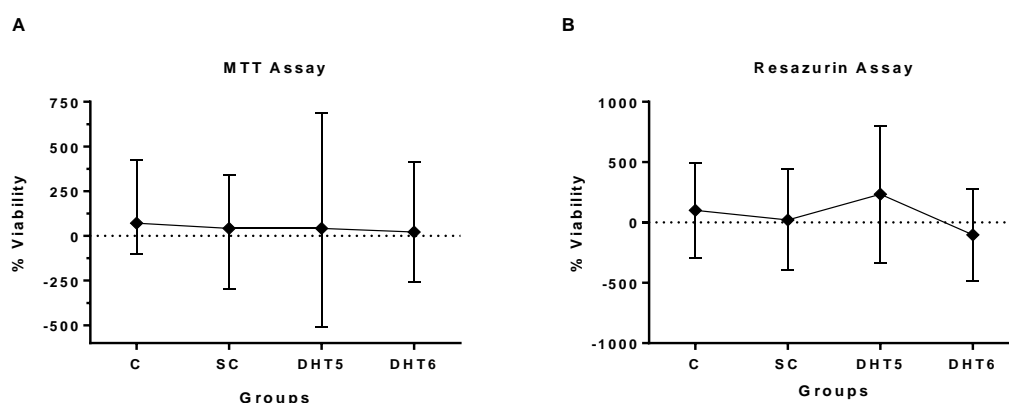
Fig. 12. Viabilities (% relative to the control) of 18-day-old brown trout primary hepatocyte spheroids after 96 h exposures to: control – C (supplemented DMEM/F-12 medium), solvent control – SC (0.1% ethanol in complete DMEM/F-12 medium), 10 μM of 5α-DHT – DHT5 and 100 μM of 5α-DHT – DHT6, using MTT (A) or resazurin (B) assays.

3.3.3 Morphology – Qualitative Analysis

H&E staining of sections from spheroids exposed to two concentrations of 5α-DHT for 96 h are represented in Fig. 13. Spheroids from the control groups had a similar structure, with intact nuclei and cellular membranes as well as spherical shapes. The outer limits of the spheroids are distinct (Fig. 13A and B). Spheroids exposed to DHT5 also displayed spherical shapes in general, with intact nuclei and membranes. However, further vacuolization was found. In the DHT6 condition, spheroids did not show spherical structures, since the hepatocytes were not compact. Only a reduced number of intact isolated cells with distinct nuclei and cellular membranes were found (Fig. 13D).
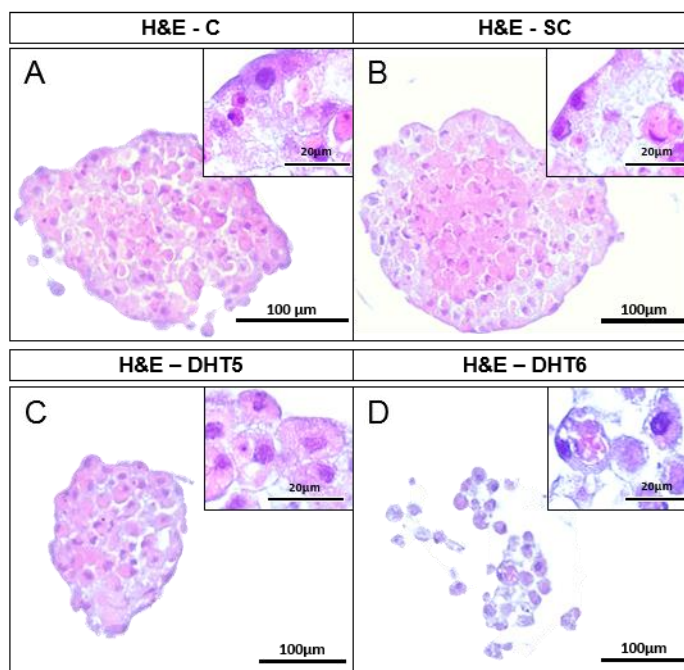
Fig. 13. Histological sections from 18-day-old brown trout spheroids after 96 h exposures to A. control – C (supplemented DMEM/F-12 medium); B. solvent control – SC (0.1% ethanol in complete DMEM/F-12 medium); C. 10 µM of 5α-DHT – DHT5 and D. 100 µM of 5α-DHT – DHT6. Paraffin sections were stained with H&E.

3.3.4 Immunohistochemistry

Immunohistochemistry with caspase-3 and E-cadherin in spheroids exposed to 5α-DHT for 96 h are demonstrated in Fig. 14. No immunostaining was observed in any of the negative controls.

For the C and SC groups, caspase-3 immunohistochemistry showed a reduced number of punctual apoptotic cells throughout the spheroids (Fig. 14A and B). Spheroids from DHT5 condition displayed a higher number of marked hepatocytes, distributed across the spheroid (Fig. 14C). Caspase-3 labelling of the spheroids exposed to DHT6 was dispersed, with a few punctual apoptotic hepatocytes (Fig. 14D).

Regarding immunohistochemistry for E-cadherin in spheroids from the C and SC, it was possible to observe the highest intensity of the antibody in the intercellular spaces, distributed across the spheroids (Fig. 14E and F). In spheroids exposed to DHT5, the intercellular spaces between hepatocytes were labelled for E-cadherin throughout the spheroid, with a slightly higher intensity in the centre. As to DHT6, a few E-cadherin labelled cells were observed.
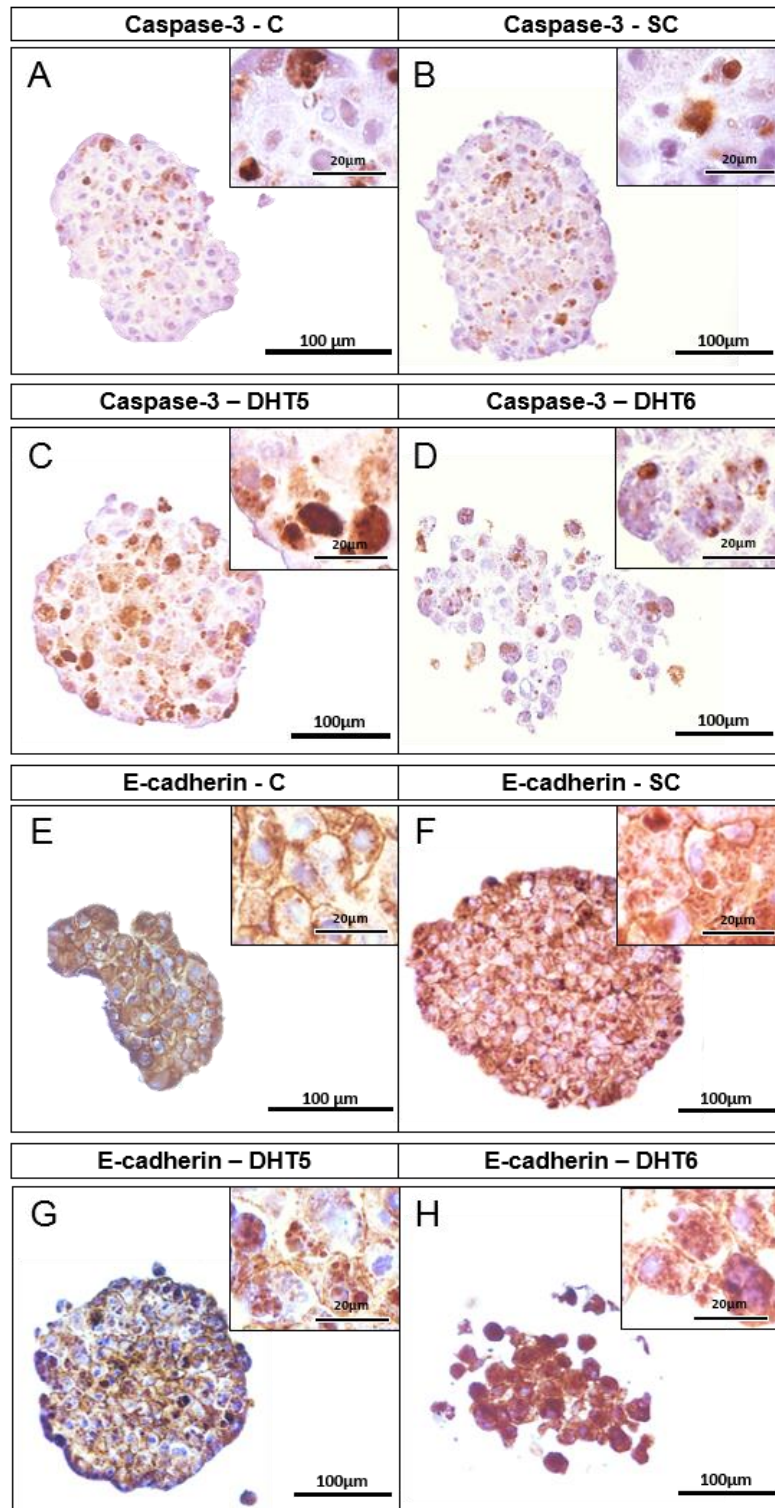
Fig. 14. Immunohistochemistry for caspase 3 (A, B, C and D) and E-cadherin (E , F, G and H) in 18-day-old brown trout spheroids after 96 h exposures to A and E. control – C (supplemented DMEM/F-12 medium); B and F. solvent control – SC (0.1% ethanol in complete DMEM/F-12 medium); C and G. 10 μM of 5α-DHT – DHT5 and D and H. 100 μM of 5α-DHT – DHT6.

3.3.5   Transmission Electron Microscopy – Ultrastructural analysis

Ultrastructure of 18-day-old spheroids after 96 h exposures to 5α-DHT is represented in Fig. 15. Hepatocytes from the control group displayed homogenous appearance throughout the spheroid. Nuclei are intact and euchromatic with prominent nucleoli, highly irregular, but rounded shapes were also observed (Fig. 15A and B). The cytoplasm revealed numerous and intact mitochondria and several rough endoplasmic reticulum (RER) cisternae. In spheroids exposed to DHT5 and DHT6 doses (Fig. 15C and D), cytoplasmic compartmentalization and integrity were lost. After DHT5 exposures, nuclei were not intact and condensed chromatin was observed at the periphery (Fig. 15C). Only a reduced number of organelles were identified in spheroids from both 5α-DHT doses, with inferior amounts in the DHT6 concentration. In spheroids exposed to the latter dose, nuclei were also scarce. Several phagocytic vesicles were noted in spheroids exposed to DHT5 and DHT6. Additionally, high electron-dense bodies were observed with variable dimensions.
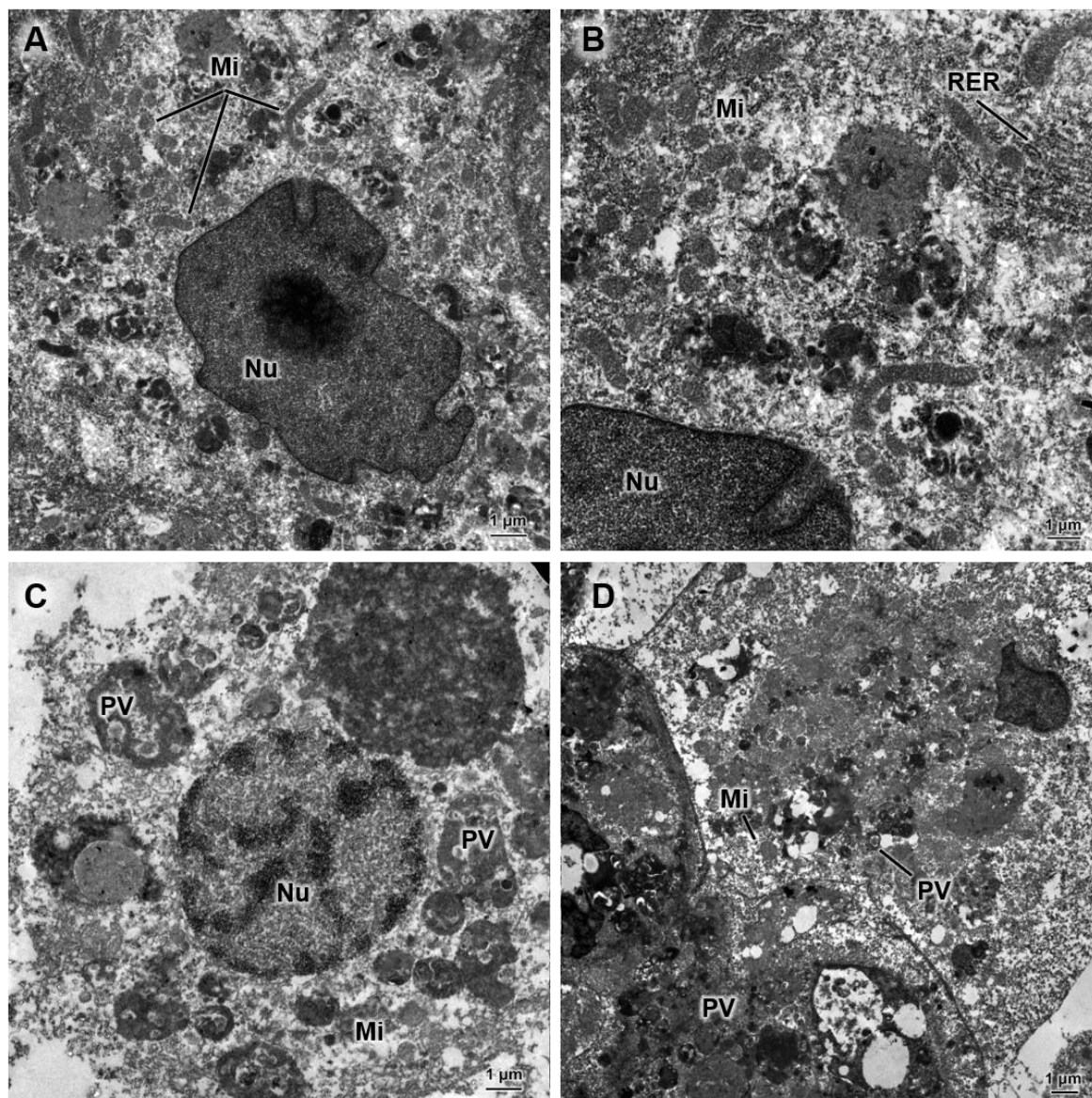
Fig. 15. TEM ultrastructure of 18-day-old brown trout primary hepatocyte spheroids after 96 h exposures to: A and B. control – C (supplemented DMEM/F-12 medium); C. 10 µM of 5α-DHT – DHT5 and D. 100 µM of 5α-DHT – DHT6. Nu – nucleus, Mi – mitochondria, RER – rough endoplasmic reticulum, PV – phagocytic vesicles.

3.3.6 Gene Expression

Relative mRNA levels of lipid metabolism-related genes in 3D cultures of brown trout primary hepatocyte spheroids exposed for 96 h to two concentrations of 5α-DHT are represented in Fig. 16. A significant decrease of *Acox1-3I* mRNA levels was observed after DHT6 exposures, in comparison to the other groups. A similar profile occurred for *PPARγ* mRNA levels. The *ApoAI* mRNA levels were not altered by 5α-DHT exposures. In contrast, both 5α-DHT doses caused a significant up-regulation of the *Acsl1* expression

levels, regarding the controls. Also, a significant increase was noted in *Fabp1* mRNA levels, but only at the highest concentration of 5α-DHT in comparison to C, SC and DHT5.
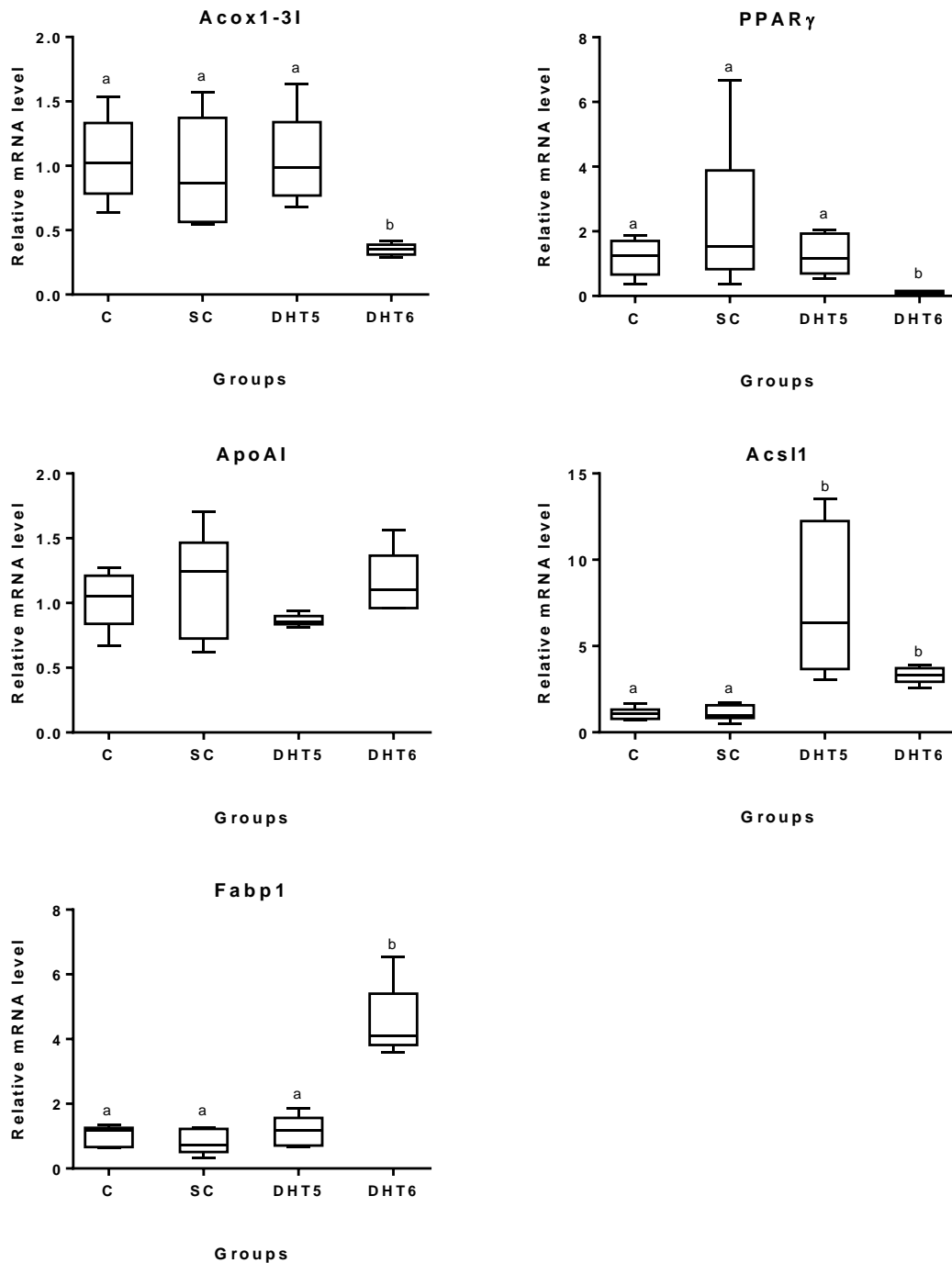
Fig. 16. Relative mRNA levels of lipid metabolism-related genes in 18-day-old brown trout primary hepatocyte spheroids after 96 h of exposure to: control – C (supplemented DMEM/F-12 medium), solvent control – SC (0.1% ethanol in complete DMEM/F-12 medium), 10 µM of 5α-DHT – DHT5 and 100 µM of 5α-DHT – DHT6. Graphical data of *Acox1-3I* (acyl-coenzyme A oxidase 1 – 3I isoform), *PPARγ* (peroxisome proliferator-activated receptor gamma), *ApoAI* (apolipoprotein AI), *Acsl1* (acyl-CoA long chain synthetase 1) and *Fabp1* (fatty acid binding protein 1) are represented as median, minimum and maximum values (42 < n ≥ 160 spheroids). Significant differences between groups are shown by different letters, according to Tuckey's pairwise parametric test or Mann-Withney with Bonferroni sequential corrections (for *Acsl1*).

55

Chapter 4. Discussion

4.1 Characterization of Brown Trout Spheroids from the Optimization Procedures

In all test conditions, after 24 h in culture, high cell density was observed and hepatocytes started to aggregate, forming heterogenous agglomerates of irregular size and shape.

For cells cultured in Leibovitz's L-15 medium without phenol red with antibiotic/antimycotic solution and FBS at 18 ºC and ±100 rpm with 2.5% p-HEMA coating (test condition IV), the aggregation process resulted in the formation of large agglomerates. By day three, almost all hepatocytes present in the wells were aggregated in a single cluster. Therefore, the suitability of coating the plates with p-HEMA for the formation of spheroids from brown trout primary hepatocytes was promptly discarded from this point. Apart from the fact that no adherent cells were found in plates from this test condition, no further advantages of culturing spheroids in p-HEMA coated plates were reported for this model.

Over time, in the remaining test conditions (I, II and III), aggregates acquired a homogenous and spherical shape, displaying defined limits and a compact appearance. Thus, the prevention of cell adhesion by the application of plate-coating polymers was not necessary for this model. In all conditions tested, around day 6, individualized hepatocytes were no longer distinguishable, and spheroids acquired a uniform appearance. This characteristic has been identified as a marker of morphological maturity of the spheroids (Baron *et al.*, 2012; Uchea *et al.*, 2015).

For spheroids cultured in test condition I, evaluation of the biometric parameters suggested a morphological stabilization on the 14th day post-isolation, according to the equivalent diameter, area and volume. Histological H&E staining analysis corroborated this feature, demonstrating spheroids with rounded and well-defined limits. Spheroids from this culture medium were the largest among all test conditions. In fact, eosinophilic centres were seen on spheroids since the 18th day. Caspase-3 IHC showed an intense marking of hepatocytes located in the centre of 18th day-old spheroids. According to literature, oxygen and nutrient diffusion might be hampered in the inner layer of spheroids in large spheroids as theses ones. This phenomenon is known to increase as a function of spheroid size. The formation of an hypoxic microenvironment was described in the core of the spheroids, which is linked to a reduction in the metabolic capacity of the cells (Asthana & Kisaalita, 2012; Langan *et al.*, 2016, 2018). Considering these facts, spheroids from this test condition might have been subjected to oxygen or nutrient deprivation after the 16th –

18th days. Therefore, the existence of viable and metabolically active cells cannot be confirmed for mature spheroids from test condition I.

In test condition II, from the 16th until the last day of culture, spheroids showed no significant variations in the equivalent diameter, area and volume, which indicates morphological stabilization, i.e. maturation. Caspase-3 IHC results demonstrated no necrotic centre formation along the culture time. Furthermore, high sphericity values were achieved since the 14th day in culture. In general, spheroids revealed high integrity and homogeneity, with distinct cellular membranes, according to H&E. Distribution of glycogen was similar between 8-day-old and 18-day-old spheroids, indicating an active and constant storage of glycogen with time. Collagen deposition appeared to increase with spheroid growth. Regarding E-cadherin IHC, an intense labelling in the intercellular spaces was across spheroids. Thus, cell-cell interactions were established. These findings corroborate the integrity of spheroids formed under this test condition.

Biometry of spheroids from test condition III displayed reduced variations on the equivalent diameter, area, volume and sphericity over the 30 days of culture. Morphometric alterations stabilized prior to any of the remaining test conditions. Spheroids were the smallest among all culture media tested, and, as expected, no necrotic cores were found. Staining techniques and IHC on paraffin sections confirm these findings, i.e, small sizes, healthy and intact cells, spherical morphological stabilization and no apoptotic cores. The drawback of the small size of these spheroids, is the fact that the sampling and the general handling was an extremely difficult and time-consuming task.

For test conditions I, II and III vacuoles were found in all time-points, with the latter culture media presenting further vacuolization. As illustrated by PAS and PAS with diastase staining, it was confirmed that some of the vacuoles were, in fact, glycogen deposits. Similar results were found in 3D cultures from PLHC-1 cell line, with distributed glycogen-rich cells in the microtissues after 8 days in culture (Rodd *et al.*, 2017). This suggests an active mobilization of lipids during spheroids' formation, as was also described for spheroids from primary human hepatocytes in co-culture with non-parenchymal cells (Messner *et al.*, 2018). This aspect confirms that lipid metabolic pathways are active and validates all test conditions for assessment of lipid-metabolism genes' expression. In this work, the presence of collagen was identified in spheroids from all culture media. MT staining showed that this structural protein was present from the first time point studied, until the last day in culture, which was verified for all test conditions. However, test condition III revealed much lower quantities than the remaining culture media. Functional hepatocyte-like spheroids (from human pluripotent stem cells) also

showed glycogen storage and collagen synthesis through histological staining (Vosough *et al.*, 2013). Cell-extracellular matrix along with cell–cell interactions are characteristic of differentiated cells, and play important roles on cellular aggregation, contributing for restoration and maintenance of liver-specific functions in cultured hepatocytes (Flouriot *et al.*, 1993; Sato *et al.*, 1989; Tzanakakis *et al.*, 2001). E-cadherin is a cell-cell adhesion molecule, required for the formation of cellular junctions. In spheroids, intercellular connections are essential for structure stability and, possibly, cell viability (Langan *et al.*, 2017; Luebke-wheeler *et al.*, 2013; Van Roy & Berx, 2008). E-cadherin epithelial marker was found with high intensities in the intercellular spaces from spheroids cultured in all test conditions. This Indicated that despite the initial enzymatic dissociation of the liver (for the isolation of primary brown trout hepatocytes), the cell-cell contacts were restored. Tight intercellular interactions were also identified through E-cadherin IHC in primary human hepatocytes in co-culture with non-parenchymal cells (Messner *et al.*, 2018).

Viability assessment through MTT and resazurin assays relies on the ability of cells to reduce the assay's components into detectable products. This capacity is only displayed by metabolically active cells, and therefore, the amount of product generated is proportional to the amount of viable cells (Riss *et al.*, 2013). High sensitivity to spheroid size was noticed in both assays used. Considering this, it is important to stress that spheroids on later days in culture had larger sizes (increased equivalent diameter, area and volume in general). This fact appears to have influenced the RFU values obtained on the resazurin assay and, to a lesser extent, the absorbance values in the MTT assay. This aspect was mainly verified for spheroids cultured in test condition I and II. Nevertheless, in both test conditions, from the first days of culture until the last, cells maintained a constant metabolic activity. According to both assays, spheroids from condition II were metabolically competent (with higher viabilities from the 18th until the 28th days)

Overall, for all the test conditions evaluated herein (test conditions I, II and III), viable, intact, homogeneous and metabolically active spheroids were maintained in culture for over 30 days. This work is the first to successfully describe, by using multiple evaluation (biometrics, morphology and viability), the formation of spheroids from brown trout primary hepatocytes, suitable for long-term applications.

4.2 Selection of the Optimal Medium and Exposure Period for Brown Trout Spheroids

The optimal culture conditions for growth of spheroids were selected as DMEM/F-12 medium with 10% (v/v) FBS, 15mM of HEPES and 10 mL/L of antibiotic/antimycotic

solution at 18 °C, without additional supply of O_2/CO_2, and at a constant agitation of ±100 rpm. Spheroids cultured in these conditions displayed metabolically active machinery, intact and healthy morphological structures, cell-cell interactions, cell-extracellular matrix interactions and active lipid-metabolism. Moreover, the equivalent diameter, area and volume achieved stability from the 16th day and the sphericity was constant since the 14th day. Necrotic centres were not identified, which suggests that nutrients and oxygen are properly diffused from the medium into the inner layers of the spheroids. Along with the stated advantages, feasibility of the spheroid's handling for experimental testing procedures also played an important role in this decision.

For the evaluation of metabolic activity of spheroids after a certain stimuli, it is important to ensure that responses are consistent. When maturity is achieved, specific functional status of the cells is stable, which guarantees reliable results. In fish spheroids, morphological stabilization was established as an indicator of maturity. Here, morphological maturation of spheroids, according to this definition, was considered to occur from 6th - 8th day post-isolation, as already occurred for fish spheroids obtained from other species (Baron *et al.*, 2017, 2012; Langan *et al.*, 2018). In this work, 8-day-old spheroids had a diameter of ± 140 μm. This value is in agreement with literature reports for fish liver cell lines (Lammel *et al.*, 2019; Langan *et al.*, 2018), and for primary hepatocytes (Hultman *et al.*, 2019; Uchea *et al.*, 2015). However, other studies reported that only from the 10th day, fish spheroids achieved maturation (Hultman *et al.*, 2019; Uchea, 2013; Uchea *et al.*, 2015). Despite the morphological stabilization, the stabilization of genetic expression might not occur on such early stages. In fact, it has been previously suggested that the stabilization of gene expression occurs in a later stage of spheroid development (Flouriot *et al.*, 1993). Until the 8th day in culture, spheroids acquired homogenous and constant morphological characteristics. Despite this morphological stability, the authors reported an irregular pattern of genetic expression in that period. In contrast, in the period after 8 days in culture, spheroids exhibited stable mRNA levels, associated with improved liver-specific functions. Such features are correlated with a proper mimicking of *in vivo* microenvironment, comprising similarities in morphological structure and genetic expression patterns with differentiated cells (Acikgöz *et al.*, 2013; Hultman *et al.*, 2019; Rodd *et al.*, 2017).

In addition, in 3D cultures from rainbow trout primary hepatocytes, the genetic expression of mature spheroids, from 10 – 25 days in culture, displayed identical patterns to those verified for the whole liver (Uchea *et al.*, 2015). These findings emphasize that an improved genetic expression potential is verified on a later stage of spheroid development. Thus, the maintenance of liver-specific functions in older spheroids was

described, which reiterates the importance of testing and maintaining the hepatocyte spheroids' viability for the maximum time in culture as possible, as was achieved here under test conditions.

Based on the few existing literature for obtaining fish hepatocyte 3D cultures, the establishment of the morphological maturation spheroids was based exclusively on the biometric parameters (mainly diameters). In this work, the assessment of spheroids' morphological stabilization was not only based on the analysis of various biometric parameters automatically, but also on the qualitative evaluation of the spheroids' cellular structure, according to histological staining techniques. Therefore, the period from the 14th until the 18th day post-isolation was identified as optimal for 96 h exposures of the spheroids to 5α-DHT. In fact, assessment of morphological changes in the fish liver cell line PLHC-1 after benzo(a)pyrene exposures is one of the few spheroid studies that reports the utilization of histology, IHC and TEM (Rodd *et al.*, 2017). However, these techniques were only performed for evaluation of exposed spheroids. No preliminary evaluation or characterisation of the spheroids was performed.

Spheroids cultured in supplemented DMEM/F-12 under the stated experimental conditions displayed relatively heterogeneous sizes and shapes. This heterogeneity is strongly correlated to the spheroids' functional capacity and structure, and has been identified as a source of variability. In order to improve the reproducibility of experiments and to achieve consistent results, a pre-selection of the spheroids according to their biometric parameters and general cellular features was proposed for spheroids from human cell-lines and applied for rainbow trout hepatocyte spheroids (Hultman *et al.*, 2019; Zanoni *et al.*, 2016). Herein we acknowledge the utility and benefits of a prior selection of the spheroids when responses to a specific impulse are being evaluated.

4.3 Exposure of 3D Spheroids from Brown Trout Primary Hepatocytes to 5α-DHT

3D exposure of brown trout primary hepatocytes to 5α-DHT had no significant influence on viability of the 18-day-old spheroids. Therefore, cells were presumed to be metabolically competent in all tested conditions. However, in both MTT and resazurin assays, the lowest viability values registered belonged to spheroids exposed to the highest 5α-DHT concentration (DHT6 – 100 μM). Thus, there was a possible impact on the metabolic activity of the cells, which is corroborated by an increase in the IHC signal of caspase-3 caused by both 5α-DHT doses.

Morphometric evaluation of the spheroids revealed no influence of exposures on the equivalent diameter, area or volume in any of the four test conditions. On the contrary, the highest concentration tested (DHT6) caused a significant decrease on the sphericity, which is in agreement with the histological observations of these spheroids. H&E suggested a disruption of the structure of cell membranes. Adhesion between cells was also compromised, since hepatocytes that appeared to have previously constituted a single spheroid were detached and isolated. Consequently, the compact 3D structure was disrupted, which goes in line with the low labelling of E-cadherin observed in spheroids from DHT6.

Regarding the ultrastructure of exposed spheroids, the difference between controls and 5α-DHT treatments was also evident. Ultrastructure of spheroids from the control group was homogeneous with numerous mitochondria, RER cisternae and intact nuclei. In addition, prominent nucleoli were found, indicative of dynamic genetic expression. These are characteristics of metabolically active hepatocytes and were reported for rainbow trout cell line RTL-W1 (Lammel *et al.*, 2019) and hepatocellular carcinoma fish cell line (Rodd *et al.*, 2017). It is suggested that spheroids were healthy and active, displaying features of differentiated fish cells (Lammel *et al.*, 2019; E Rocha *et al.*, 1994).

Following DHT5 exposures, condensed chromatin was identified at the periphery of the nucleus, indicative of cellular death (Elmore, 2007). DHT6 exposed spheroids showed a lack of structural integrity with scarce organelles and nuclei. High electron-dense bodies were found in spheroids from both 5α-DHT doses, but larger dimensions of these structures were noticed in DHT6 condition. Phagocytic vesicles were found alongside with the dense bodies and might be indicative of autophagy. In that case, cellular components are degraded by lysosomal sequestration, for recycling of the damaged materials (Ding, 2010; Moore *et al.*, 2008). This process might explain the limited number of organelles found in spheroids from exposed groups. Therefore, it is hypothesized that the electron-dense bodies and vesicles were autophagic components. Similar structures were reported in the ultrastructure of spheroids from the rainbow trout cell line RTL-W1 (Lammel *et al.*, 2019) and from human cancer cell lines (Malhão *et al.*, 2013). Autophagic processes can serve several goals in the liver, such as cell organelle reorganization, regulation of lipid homeostasis, as well as, removal of misfolded proteins (Ding, 2010; Scaff & Scussel, 2008).

TEM on spheroids from fish hepatocytes are scarce and limited to fish cell-lines. Herein, it is demonstrated that ultrastructural analysis is essential and decisive in the evaluation of the integrity and architecture of the cells and its organelles. Hence, to our

knowledge, this is the first work providing the ultrastructure of spheroids from fish primary hepatocytes.

4.4 Gene Expression after 5α-DHT Exposures

4.4.1. Effects on 2D Brown Trout Primary Hepatocytes

For 2D cultures of primary hepatocytes, exposures to six 5α-DHT doses revealed changes on the expression patterns of two of the lipid metabolism-related target genes. Selection of 5α-DHT concentrations was based on previous studies of this androgen's influence on human prostate cancer cells (Olokpa *et al.*, 2016) and mouse pluripotent cells (Singh *et al.*, 2003). In this work, mRNA levels of *Acox1-3l,* involved in peroxisomal β-oxidation, and *PPARγ*, regulator of lipid metabolism, were not influenced by androgenic exposures.

The main component of HDL lipoproteins, *ApoAI* expression values were not altered in any of the concentrations tested. In the common carp, *ApoAI* was suggested to modulate growth and development (Wang *et al.*, 2016). *ApoAI* is also involved in immune responses (Sahoo *et al.*, 2017), with suppressed expression after bacterial infection in catfish, and antimicrobial activity in the common carp (Concha *et al.*, 2004).

Acsl1 was up-regulated after monolayer primary hepatocytes exposures to DHT4, DHT5 and DHT6 doses, in a concentration-dependent manner. *Acsl1* catalyses the initial step for fatty acid turnover (Lopes-Marques *et al.*, 2013), and the results suggest an increase of long chain fatty acid (LCFA) activation, possibly followed by β-oxidation. *Acsl1* expression in grass carp was tissue-dependent and down-regulated by fat diets (Cheng *et al.*, 2017). The authors suggest that Acsl1 proteins catalyse the acylation of endogenous or exogenous fatty acids, depending on the transcript variant of the gene. Acsl1 plays important roles in the LCFA uptake in the heart (Grevengoed *et al.*, 2015), influenced by female ovarian hormones in mice (Goldenberg *et al.*, 2016).

Increased mRNA levels of *Fabp1* were observed after DHT6 exposure. High expression of this transport protein implies a rise in FA aggregation with the Fabp1 for transport facilitation into the liver (Amiri *et al.*, 2018), Similarly, in "chang liver" cells, overexpression of human *Fabp1* resulted in an uptake of LCFA (Gao *et al.*, 2010). Clofibrate (a lipid lowering drug) increased *Fabp1* expression, suggesting that interactions between Fabp1 and PPARs are likely to occur (Wolfrum *et al.*, 2001).

In vitro effects caused by different androgens in fish lipid pathways are scarce. These concern 11-KT exposures of coho salmon, that resulted in ovarian follicle

development and potential alteration of lipid metabolism pathways (Monson *et al.*, 2017); and rainbow trout following exposures to 17β-estradiol, T and 5α-DHT (Cleveland & Weber, 2016). The latter induced no alteration on gene expression, however, 5α-DHT's response might be mediated by different genes and mechanisms, not evaluated by the authors. Considering the results for 2D cultures, DHT5 and DHT6 appeared to induce alterations in the mRNA levels of two target genes. Therefore, these were considered to be the most promising 5α-DHT concentrations for further evaluation and comparison on the following 3D assays.

4.4.2. Effects on 3D Brown Trout Primary Hepatocytes and Comparison with 2D Cultures

Regarding the viabilities of 2D cultures of primary hepatocytes, no significant differences between any of the tested conditions in comparison to control were found. However, the minimum values registered according to the Trypan blue exclusion assay were recorded for cells exposed to highest dose (100 μm), and these wells revealed decreased cellularity with time in culture. Similarly to the 3D results, the cells from the DHT6 dose were less aggregated between each other. Thus, 5α-DHT at the highest dose appears to exert some influence in the aggregation and amount of hepatocytes, with possible, but non-significant, influences on the viability.

Brown trout primary hepatocyte spheroids demonstrated higher sensitivity to 5α-DHT exposures, comparing with 2D results. In contrast to 2D effects, the peroxisomal targets, *Acox1-3I* and *PPARγ*, were similarly influenced by DHT6 exposure, with a decrease on mRNA levels. *Acox1-3I* is the first rate-limiting enzyme of peroxisomal β-oxidation, an both splicing isoforms display conservative roles in vertebrate fatty acid metabolism (He *et al.*, 2014; Madureira *et al.*, 2016a). Investigation on this topic is focused on 2D *in vitro* experiments. Tissue specificity in *Acox1-3I* modulation was found in zebrafish, as well as, up-regulation following feeding, also verified for rainbow trout (Morais *et al.*, 2007). Similarly, along with tissue-specific functions, nutritional status was proposed to modulate the expression of each isoform in Nile tilapia (He *et al.*, 2014). In brown trout spheroids, the down-regulation observed directly suggests a reduction in the conversion of LCFA to very-LCFA. In the common carp, clofibrate exposures resulted in increased levels of *Acox1-3I* (Corcoran *et al.*, 2015), this up-regulation was also observed after fibrates' exposure of Atlantic salmon hepatocytes (Ruyter *et al.*, 1997). Along with these studies, suggestion of cross-links to PPARs were also found in mice (Vluggens *et al.*, 2010).

The decrease on mRNA levels observed for *PPARγ* expression is likely to result in alterations on lipid and FA storage, as well as in the regulation of adipogenesis This gene was proposed to mediate dietary regulation of fatty acid bioconversion enzymes in the liver of the rainbow trout (Kamalam *et al.*, 2013). Similar results were found for human prostate cancer cell lines exposed to 5α-DHT, with a down-regulation in a time and concentration dependent-manner, even for lower concentrations (1 -10 nM) (Olokpa *et al.*, 2016). Also in agreement with these findings, decreased *PPARγ* levels in mouse pre-adipocytes and pluripotent cells exposed to 5α-DHT appeared to be mediated through AR activation. In result, suppression of adipocyte differentiation was found, with consequences at lipid storage level (Singh *et al.*, 2003). In primary brown trout hepatocytes exposed to both estrogenic and androgenic stimuli, *PPARγ* mRNA levels decreased, suggesting interconnection with ER and AR (Lopes *et al.*, 2016). In Nile tilapia, *PPARγ* was highly expressed in the liver and, in order to exert their actions on target genes, a collaboration with different receptors is proposed (He *et al.*, 2015). Acox1 is known to be a weak peroxisome proliferative responder (Corcoran *et al.*, 2015; Madureira *et al.*, 2016a), thus, the concordance between results of the expression of these genes.

The 3D results for *PPARγ* and *Acox1-3l* were in contrast with the 2D that revealed decreased sensitivity in this case, as opposed to the literature reports above-mentioned. An under-estimation of the influence of 5α-DHT on primary hepatocytes' expression in monolayer cultures is suggested, with negative consequences on the assessment of the pathways influenced by this androgen. *ApoAI* gene expression was not altered in any of the concentrations tested, as observed in the 2D experiments.

Up-regulation of *Acsl1* mRNA levels was observed, after exposures to both DHT5 and DHT6 doses. This corroborates the 2D results, reinforcing the probability of increased LCFA activation for energy production through redirection into β-oxidation by Acsl1 proteins (Cheng *et al.*, 2017).

Similarly, *Fabp1* up-regulated expression patterns for 3D hepatocytes cultures were comparable to those observed for 2D hepatocyte cultures. In both cases, an increase of LCFA transportation into the liver is apparent, implying that at high doses (DHT6), 5α-DHT influenced the regulation of intercellular storage of FA, via this transport protein (Wang *et al.*, 2015).

Evaluation of the genetic expression of 2D and 3D primary hepatocytes following 5α-DHT exposures points towards alterations on lipidic pathways related to LCFA activation, transport into the liver and redirection of lipids and FA for anabolic of catabolic reactions. Therefore, the inclusion of further targets is projected in future experimental

efforts, including: (1) Lipoprotein lipase (*lpl*) involved in the hydrolysis of TG from the core of chylomicrons and VLDLs into free FA (Urbatzka *et al.*, 2015), since evidences of regulation by 11-Ketotostosterone were found in the ovaries of shortfinned eel (Divers *et al.*, 2010); (2) Steroidogenic acute regulatory protein (*StAR*) for the facilitation of cholesterol in early gonadal steroidogenesis (Faheem *et al.*, 2017; Kusakabe *et al.*, 2006; Nakamura *et al.*, 2005) and (3) Fatty acid synthetase (*Fasn*) for FA synthesis and oxidation (Cunha *et al.*, 2013;). This work confirms the proximity of 3D cultures with *in vivo* data, constituting an advantage concerning 2D cultures. Not only spheroids mimic cellular structure and organization, but also cell differentiation with restoration of liver-specific functions and genetic expression patterns. As was previously suggested, genetic expression of spheroids seems to be comparable to that of the whole liver in the case the rainbow trout (Uchea *et al.*, 2013). Thus, emphasizing the necessity and utility of 3D cultures in the accurate evaluation of hormonal and EDCs effects in fish.

Chapter 5. Conclusions

Summing up, with this study we were able to optimize the best condition for culturing and maintaining 3D spheroids from brown trout primary hepatocytes, as: DMEM/F-12 medium with 10% (v/v) FBS, 15mM of HEPES and 10 mL/L of antibiotic/antimycotic solution at 18 ºC, without additional supply of O_2/CO_2, and at a constant agitation of ±100 rpm. Spheroids acquired morphological maturity around the 6th - 8th days post-isolation, and were maintained viable until 30 days in culture. Under these culture conditions, 3D exposures to 5α-DHT (at 10 and 100 µM) caused altered gene expressions in four of the lipidic target genes tested (*Acox1-3l*, *PPARγ*, *Acsl1* and *Fabp1*). Comparatively, at the same doses, brown trout hepatocytes cultured in 2D were affected to a lesser extent (with differences in only two of the genes tested) than hepatocytes in 3D, although the results point in the same direction. This fact reiterates the importance of testing models closer to *in vivo*, as otherwise the effects may be underestimated.

The present data is extremely relevant to reinforce the importance of the study of androgenic compounds in the lipidic metabolic pathways and their consequences, for example, in the reproductive physiology of fish, since most works in the literature focus mainly on the effects caused by estrogenic compounds. To obtain a more complete picture of the various lipidic pathways that can be altered by 5α-DHT, the inclusion of other target genes is projected in future experimental work.

Chapter 6. Bibliography

Acikgöz, A., Giri, S., Cho, M. G., & Bader, A. (2013). Morphological and functional analysis of hepatocyte spheroids generated on poly-HEMA-treated surfaces under the influence of fetal calf serum and nonparenchymal cells. *Biomolecules*, *3*(1), 242–269.

Amiri, M., Yousefnia, S., Seyed Forootan, F., Peymani, M., Ghaedi, K., & Nasr Esfahani, M. H. (2018). Diverse roles of fatty acid binding proteins (FABPs) in development and pathogenesis of cancers. *Gene*, *676*(May), 171–183.

Arts, M. T., & Kohler, C. (2009). Health and Condition in Fish: The Influence of Lipids on Membrane Competency and Immune Response. In M. Kainz, M. Brett, & M. Arts (Eds.), *Lipids in Aquatic Ecosystems* (pp. 237–255). Springer, New York, NY.

Asthana, A., & Kisaalita, W. S. (2012). Microtissue size and hypoxia in HTS with 3D cultures. *Drug Discovery Today*, *17*(15–16), 810–817.

Ayisi, C. L., Yamei, C., & Zhao, J. L. (2018). Genes, transcription factors and enzymes involved in lipid metabolism in fin fish. *Agri Gene*, *7*, 7–14.

Bachmann, A., Moll, M., Gottwald, E., Nies, C., Zantl, R., Wagner, H., Burkhardt, B., Sánchez, J. J. M, Ladurner, R., Thasler, W., Damm, G. & Nussler, A. (2015). 3D Cultivation Techniques for Primary Human Hepatocytes. *Microarrays*, *4*, 64–83.

Baron, M. G., Mintram, K. S., Owen, S. F., Hetheridge, M. J., Moody, A. J., Purcell, W. M., Jackson, S. K. & Jha, A. N. (2017). Pharmaceutical metabolism in fish: Using a 3-D hepatic *in vitro* model to assess clearance. *PLoS ONE*, *12*(1), 1–13.

Baron, M. G., Purcell, W. M., Jackson, S. K., Owen, S. F., & Jha, A. N. (2012). Towards a more representative in vitro method for fish ecotoxicology: Morphological and biochemical characterisation of three-dimensional spheroidal hepatocytes. *Ecotoxicology*, *21*(8), 2419–2429.

Borg, B. (1994). Androgens in teleost fishes. *Comparative Biochemistry and Physiology. Part C: Toxicology and Pharmacology*, *109*(3), 219–245.

Brockmeier, E. K., Jayasinghe, B. S., Pine, W. E., Wilkinson, K. A., & Denslow, N. D. (2014). Exposure to paper mill effluent at a site in north central florida elicits molecular-level changes in gene expression indicative of progesterone and androgen exposure. *PLoS ONE*, *9*(9), e106644.

Cheng, H. L., Chen, S., Xu, J. H., Yi, L. F., Peng, Y. X., Pan, Q., Shen, X., Dong, Z.,

Zhang, X. & Wang, W. (2017). Molecular cloning and nutrient regulation analysis of long chain acyl-CoA synthetase 1 gene in grass carp, *Ctenopharyngodon idella L. Comparative Biochemistry and Physiology Part - B: Biochemistry and Molecular Biology*, *204*, 61–68.

Cleveland, B. M., & Weber, G. M. (2016). Effects of steroid treatment on growth, nutrient partitioning, and expression of genes related to growth and nutrient metabolism in adult triploid rainbow trout (*Oncorhynchus mykiss*). *Domestic Animal Endocrinology*, *56*, 1–12.

Collett, G. P., Betts, A. M., Johnson, M. I., Pulimood, A. B., Cook, S., Neal, D. E., & Robson, C. N. (2000). Peroxisome proliferator-activated receptor α is an androgen-responsive gene in human prostate and is highly expressed in prostatic adenocarcinoma. *Clinical Cancer Research*, *6*(8), 3241–3248.

Concha, M. I., Smith, V. J., Castro, K., Bastías, A., Romero, A., & Amthauer, R. J. (2004). Apolipoproteins A-I and A-II are potentially important effectors of innate immunity in the teleost fish *Cyprinus carpio*. *European Journal of Biochemistry*, *271*(14), 2984–2990.

Corcoran, J., Winter, M. J., Lange, A., Cumming, R., Owen, S. F., & Tyler, C. R. (2015). Effects of the lipid regulating drug clofibric acid on PPARα-regulated gene transcript levels in common carp (*Cyprinus carpio*) at pharmacological and environmental exposure levels. *Aquatic Toxicology*, *161*, 127–137.

Cravedi, J. P., Paris, A., Monod, G., Devaux, A., Flouriot, G., & Valotaire, Y. (1996). Maintenance of cytochrome P450 content and phase I and phase II enzyme activities in trout hepatocytes cultured as spheroidal aggregates. *Comparative Biochemistry and Physiology - C Pharmacology Toxicology and Endocrinology*, *113*(2), 241–246.

Cunha, I., Galante-oliveira, S., Rocha, E., Planas, M., Urbatzka, R., & Castro, L. F. C. (2013). Dynamics of PPARs, fatty acid metabolism genes and lipid classes in eggs and early larvae of a teleost. *Comparative Biochemistry and Physiology Part B*, *164*, 247–258.

De Falco, M., Forte, M., & Laforgia, V. (2015). Estrogenic and anti-androgenic endocrine disrupting chemicals and their impact on the male reproductive system. *Frontiers in Environmental Science*, *3*, 3.

Denizot, F., & Lang, R. (1986). Rapid colorimetric assay for cell growth and survival - Modifications to the tetrazolium dye procedure giving improved sensitivity and

reliability. *Journal of Immunological Methods*, *89*(2), 271–277.

Dickhoff, W. W., Brown, C. L., Sullivan, C. V, & Bern, H. A. (1990). Fish and amphibian models for developmental endocrinology. *Journal of Experimental Zoology*, *256*(S4), 90–97.

Ding, W. (2010). Role of autophagy in liver physiology and pathophysiology. *World Journal of Biological Chemistry*, *1*(1), 3–12.

Divers, S. L., Mcquillan, H. J., Matsubara, H., Todo, T., & Lokman, P. M. (2010). Effects of reproductive stage and 11-ketotestosterone on LPL mRNA levels in the ovary of the shortfinned eel. *Journal of Lipid Research*, *51*, 3250–3258.

Eilenberger, C., Rudi, S., Kratz, A., Rothbauer, M., Ehmoser, E., & Ertl, P. (2018). Optimized alamarBlue assay protocol for drug dose-response determination of 3D tumor spheroids. *MethodsX*, *5*, 781–787.

Elmore, S. (2007). Apoptosis: A Review of Programmed Cell Death. *Toxicologic Pathology*, *35*(4), 495–516.

Endo, T., Todo, T., Lokman, P. M., Kudo, H., Ijiri, S., Adachi, S., & Yamauchi, K. (2011). Androgens and very low density lipoprotein are essential for the growth of previtellogenic oocytes from japanese eel, *Anguilla japonica*, *in vitro. Biology of Reproduction*, *84*(4), 816–825.

Faheem, M., Khaliq, S., & Lone, K. P. (2017). Disruption of the reproductive axis in freshwater fish, *Catla catla* , after bisphenol-a exposure . *Zoological Science*, *34*(5), 438–444.

Fay, K. A., Mingoia, R. T., Goeritz, I., Nabb, D. L., Ho, A. D., Ferrell, B. D., Peterson, H. M., Nichols, J. W., Segner, H. & Han, X. (2014). Intra- and interlaboratory reliability of a cryopreserved trout hepatocyte assay for the prediction of chemical bioaccumulation potential. *Environmental Science and Technology*, *48*, 8170–8178.

Flouriot, G., Vaillant, C., Salbert, G., Pelissero, C., Guiraud, J. M., & Valotaire, Y. (1993). Monolayer and aggregate cultures of rainbow trout hepatocytes: long-term and stable liver-specific expression in aggregates. *Journal of Cell Science*, *105,* 407–416.

Forbes, E., & Lokman, P. (2011). Lipid stock-piling in the growing oocyte - are androgens driving lipid delivery to sustain the future embryo of the eel, *Anguilla australis*? *Indian Journal of Science and Technology*, *4*(S8), 175.

Gao, N., Qu, X., Yan, J., Huang, Q., Yuan, H.-Y., & Ouyang, D.-S. (2010). L-FABP T94A

decreased fatty acid uptake and altered hepatic triglyceride and cholesterol accumulation in Chang liver cells stably transfected with L-FABP. *Molecular and Cellular Biochemistru, 345*, 207–214.

Goldenberg, J. R., Wang, X., & Lewandowski, E. D. (2016). Acyl CoA synthetase-1 links facilitated long chain fatty acid uptake to intracellular metabolic trafficking differently in hearts of male versus female mice. *Journal of Molecular and Cellular Cardiology*, *94*, 1–9.

Grevengoed, T. J., Martin, S. A., Katunga, L., Cooper, D. E., Anderson, E. J., Murphy, R. C., & Coleman, R. A. (2015). Acyl-CoA synthetase 1 deficiency alters cardiolipin species and impairs mitochondrial function. *Journal of Lipid Research*, *56*(8), 1572–1582.

Han, X., Mingoia, R. T., Nabb, D. L., Yang, C., Snajdr, S. I., & Hoke, R. A. (2008). Xenobiotic intrinsic clearance in freshly isolated hepatocytes from rainbow trout (*Oncorhynchus mykiss*): Determination of trout hepatocellularity , optimization of cell concentrations and comparison of serum and serum-free incubations. *Aquatic Toxicology*, *89*, 11–17.

He, A. Y., Liu, C. Z., Chen, L. Q., Ning, L. J., Qin, J. G., Li, J. M. & Du, Z. Y. (2015). Molecular characterization, transcriptional activity and nutritional regulation of peroxisome proliferator activated receptor gamma in Nile tilapia (*Oreochromis niloticus*). *General and Comparative Endocrinology*, *223*, 139–147.

He, A. Y., Liu, C. Z., Chen, L. Q., Ning, L. J., Zhang, M. L., Li, E. C., & Du, Z. Y. (2014). Identification, characterization and nutritional regulation of two isoforms of acyl-coenzyme A oxidase 1 gene in Nile tilapia (*Oreochromis niloticus*). *Gene*, *545*(1), 30–35.

Higgs, D. ., & Dong, F. . (2000). Lipids and Fatty Acids. In R. R. Stickney (Ed.), *The Encyclopedia of Aquaculture* (pp. 476–496). John Wiley and Sons Inc. New York.

Ho, W. Y., Yeap, S. K., Ho, C. L., Rahim, R. A., & Alitheen, N. B. (2012). Development of multicellular tumor spheroid (MCTS) culture from breast cancer cell and a high throughput screening method using the MTT Assay. *PLoS ONE*, *7*(9), e44640.

Hultman, M. T., Løken, K. B., Grung, M., Reid, M. J., & Lillicrap, A. (2019a). Performance of three-dimensional rainbow trout (*Oncorhynchus mykiss*) hepatocyte spheroids for evaluating biotransformation of pyrene. *Environmental Toxicology and Chemistry*, *38*(8), 1738–1747.

Hultman, M. T., Løken, K. B., Grung, M., Reid, M. J., & Lillicrap, A. (2019b). Performance of three-dimensional rainbow trout (*Oncorhynchus mykiss*) hepatocyte spheroids for evaluating biotransformation of pyrene. *Environmental Toxicology and Chemistry*, *38*(8), 1738–1747.

Hussain, R. F., Nouri, A. M. E., & Oliver, R. T. D. (1993). A new approach for measurement of cytotoxicity using colorimetric assay. *Journal OfImmunological Methods*, *160*, 89–96.

Imamichi, Y., Yuhki, K. I., Orisaka, M., Kitano, T., Mukai, K., Ushikubi, F., Taniguchi, T., Umezawa, A. Miyamoto, K. & Yazawa, T. (2016). 11-Ketotestosterone is a major androgen produced in human gonads. *Journal of Clinical Endocrinology and Metabolism*, *101*(10), 3582–3591.

Ivanov, D. P., Grabowska, A. M., & Garnett, M. C. (2017). Cell Viability Assays: Methods and protocols. In D. Gilbert & O. Friedrich (Eds.), *Methods in Molecular Biology* (Vol. 1601, pp. 43–59).

Ivanov, D. P., Parker, T. L., Walker, D. A., Alexander, C., Ashford, M. B., Gellert, P. R., & Garnett, M. C. (2014). Multiplexing spheroid volume , resazurin and acid phosphatase viability assays for high-throughput screening of tumour spheroids and stem cell neurospheres. *PLoS ONE*, *9*(8), e103817.

José Ibáñez, A., Peinado-Onsurbe, J., Sánchez, E., Cerdá-Reverter, J. M., & Prat, F. (2008). Lipoprotein lipase (LPL) is highly expressed and active in the ovary of European sea bass (Dicentrarchus labrax L.), during gonadal development. *Comparative Biochemistry and Physiology - A Molecular and Integrative Physiology*, *150*(3), 347–354.

Kamalam, B., Médale, F., Larroquet, L., Corraze, G., & Panserat, S. (2013). Metabolism and fatty acid profile in fat and lean rainbow trout lines fed with vegetable oil : effect of carbohydrates. *PLOS One*, *8*(10), e76570.

Kinnberg, K., & Toft, G. (2003). Effects of estrogenic and antiandrogenic compounds on the testis structure of the adult guppy (*Poecilia reticulata*). *Ecotoxicology and Environmental Safety*, *54*(1), 16–24.

Kleveland, E. J., Ruyter, B., Vegusdal, A., Sundvold, H., Berge, R. K., & Gjøen, T. (2006). Effects of 3-thia fatty acids on expression of some lipid related genes in Atlantic salmon (*Salmo salar L.*). *Comparative Biochemistry and Physiology - B Biochemistry and Molecular Biology*, *145*(2), 239–248.

Kozyra, M., Johansso, I., Nordling, Å., Ullah, S., Lauschke, V. M., & Ingelman-sundberg, M. (2018). Human hepatic 3D spheroids as a model for steatosis and insulin resistance. *Scientific Reports*, *8*(14297), 1–12.

Kusakabe, M., Nakamura, I., Evans, J., Swanson, P., & Young, G. (2006). Changes in mRNAs encoding steroidogenic acute regulatory protein, steroidogenic enzymes and receptors for gonadotropins during spermatogenesis in rainbow trout testes. *Journal of Endocrinology*, *189*(3), 541–554.

Lammel, T., Tsoukatou, G., Jellinek, J., & Sturve, J. (2019). Development of three-dimensional (3D) spheroid cultures of the continuous rainbow trout liver cell line RTL-W1. *Ecotoxicology and Environmental Safety*, *167*, 250–258.

Langan, L. M., Dodd, N. J. F., Owen, S. F., Purcell, W. M., Jackson, S. K., & Jha, A. N. (2016). Direct measurements of oxygen gradients in spheroid culture system using electron paramagnetic resonance oximetry. *PLoS ONE*, *11*(8), 1–13.

Langan, L. M., Harper, G. M., Owen, S. F., Purcell, W. M., Jackson, S. K., & Jha, A. N. (2017). Application of the rainbow trout derived intestinal cell line (RTgutGC) for ecotoxicological studies : molecular and cellular responses following exposure to copper. *Ecotoxicology*, 1117–1133.

Langan, L. M., Owen, S. F., Trznadel, M., Dodd, N. J. F., Jackson, S. K., Purcell, W. M., & Jha, A. N. (2018). Spheroid size does not impact metabolism of the β-blocker propranolol in 3D intestinal fish model. *Frontiers in Pharmacology*, *9*, 1–10.

Leaver, M. J., Bautista, J. M., Björnsson, B. T., Jönsson, E., Krey, G., Tocher, D. R., & Torstensen, B. E. (2008). Towards fish lipid nutrigenomics: Current state and prospects for fin-fish aquaculture. *Reviews in Fisheries Science*, *16*(S1), 73–94.

Lee, S. M. L., Schelcher, C., Demmel, M., Hauner, M., & Thasler, W. E. (2013). Isolation of Human Hepatocytes by a Two-step Collagenase Perfusion Procedure. *Journal of Visualized Experiments*, (79), e50615.

Li, Y., Gao, M., Wu, D., & Bao, J. (2017). Isolations and Cultures of Primary Hepatocytes. *Clinical & Experimental Pathology*, *7*(5), 1–4.

Lopes-Marques, M., Cunha, I., Reis-Henriques, M. A., Santos, M. M., & Castro, L. F. C. (2013). Diversity and history of the long-chain acyl-CoA synthetase (Acsl) gene family in vertebrates. *BMC Evolutionary Biology*, *13*(271), 1471–2148.

Lopes, C., Madureira, T. V., Ferreira, N., Pinheiro, I., Castro, L. F. C., & Rocha, E. (2016). Peroxisome proliferator-activated receptor gamma (PPARγ) in brown trout:

Interference of estrogenic and androgenic inputs in primary hepatocytes. *Environmental Toxicology and Pharmacology*, *46*, 328–336.

Lopes, C., Malhão, F., Guimarães, C., Pinheiro, I., Gonçalves, J. F., Castro, L. F. C., Rocha, E. & Madureira, T. V. (2017). Testosterone-induced modulation of peroxisomal morphology and peroxisome-related gene expression in brown trout (*Salmo trutta* f. *fario*) primary hepatocytes. *Aquatic Toxicology*, *193*, 30–39.

Luebke-wheeler, J. L., Nedredal, G., Yee, L., Amiot, B., & Nyberg, S. (2013). E-Cadherin protects primary hepatocyte spheroids from cell death by a caspase-independent mechanism. *Cell Transplant*, *18*(12), 1281–1287.

Madureira, T. V., Castro, L. F. C., & Rocha, E. (2016a). Acyl-coenzyme A oxidases 1 and 3 in brown trout (*Salmo trutta* f. *fario*): Can peroxisomal fatty acid β-oxidation be regulated by estrogen signaling? *Fish Physiology and Biochemistry*, *42*(1), 389–401.

Madureira, T. V., Castro, L. F. C., & Rocha, E. (2016b). Acyl-coenzyme A oxidases 1 and 3 in brown trout (*Salmo trutta* f. *fario*): Can peroxisomal fatty acid β-oxidation be regulated by estrogen signaling? *Fish Physiology and Biochemistry*, *42*(1), 389–401.

Madureira, T. V., Malhão, F., Pinheiro, I., Lopes, C., Ferreira, N., Urbatzka, R., Castro, L. F. C & Rocha, E. (2015). Estrogenic and anti-estrogenic influences in cultured brown trout hepatocytes: Focus on the expression of some estrogen and peroxisomal related genes and linked phenotypic anchors. *Aquatic Toxicology*, *169*, 133–142.

Madureira, T. V., Malhão, F., Simões, T., Pinheiro, I., Lopes, C., Gonçalves, J. F., Lemos, M. F. L. & Rocha, E. (2018). Sex-steroids and hypolipidemic chemicals impacts on brown trout lipid and peroxisome signaling — Molecular, biochemical and morphological insights. *Comparative Biochemistry and Physiology Part - C: Toxicology and Pharmacology, 212*, 1–17.

Madureira, T. V., Pinheiro, I., Malhão, F., Lopes, C., Urbatzka, R., Castro, L. F. C., & Rocha, E. (2017). Cross-interference of two model peroxisome proliferators in peroxisomal and estrogenic pathways in brown trout hepatocytes. *Aquatic Toxicology*, *187*, 153–162.

Malhão, F., Urbatzka, R., Navas, J. M., Cruzeiro, C., Monteiro, R. A. F., & Rocha, E. (2013). Tissue and Cell Cytological , immunocytochemical , ultrastructural and growth characterization of the rainbow trout liver cell line RTL-W1. *Tissue and Cell*, *45*(3), 159–174.

Matsumoto, T., Sakari, M., Okada, M., Yokoyama, A., Takahashi, S., Kouzmenko, A., &

Kato, S. (2013). The androgen receptor in health and disease. *Annual Review of Physiology*, *75*, 201–224.

Mayes, J. S., & Watson, G. H. (2004). Direct effects of sex steroid hormones on adipose tissues and obesity. *Obesity Reviews*, *5*(4), 197–216.

Messner, S., Fredriksson, L., Lauschke, V. M., Roessger, K., Escher, C., Bober, M., Kelm, J. M., Ingelman-Sundberg, M. & Moritz, W. (2018). Transcriptomic, proteomic, and functional long-term characterization of multicellular three-dimensional human liver microtissues. *Applied In Vitro Toxicology*, *4*(1), 1–12.

Milla, S., Depiereux, S., & Kestemont, P. (2011). The effects of estrogenic and androgenic endocrine disruptors on the immune system of fish: A review. *Ecotoxicology (London, England)*, *20*, 305–319.

Monroig, O., Tocher, D. R., & Castro, L. F. C. (2018). Polyunsaturated fatty acid biosynthesis and metabolism in fish. In G. C. Burdge (Ed.), *Polyunsaturated Fatty Acid Metabolism* (pp. 31–60).

Monson, C., Forsgren, K., Goetz, G., Harding, L., Swanson, P., & Young, G. (2017). A teleost androgen promotes development of primary ovarian follicles in coho salmon and rapidly alters the ovarian transcriptome. *Biology of Reproduction*, *97*(5), 731–745.

Moore, M. N., Koehler, A., Lowe, D., & Viarengo, A. (2008). Lysosomes and Autophagy in Aquatic Animals. In *Methods in Enzymology* (Vol. 451, pp. 581–620).

Morais, S., Knoll-Gellida, A., André, M., Barthe, C., & Babin, P. J. (2007). Conserved expression of alternative splicing variants of peroxisomal acyl-CoA oxidase 1 in vertebrates and developmental and nutritional regulation in fish. *Physiological Genomics*, *28*(3), 239–252.

Mosmann, T. (1983). Rapid colorimetric assay for cellular growth and survival: Application to proliferation and cytotoxicity assays. *Journal of Immunological Methods*, *65*(1–2), 55–63.

Nakamura, I., Evans, J. C., Kusakabe, M., Nagahama, Y., & Young, G. (2005). Changes in steroidogenic enzyme and steroidogenic acute regulatory protein messenger RNAs in ovarian follicles during ovarian development of rainbow trout (*Oncorhynchus mykiss*). *General and Comparative Endocrinology*, *144*(3), 224–231.

Nakamura, M. T., & Nara, T. Y. (2004). Structure , function, and dietary regulation of Δ6, Δ5, and Δ9 desaturases. *Annual Review of Nutrition*, *24*, 345–376.

Olokpa, E., Bolden, A., & Stewart, L. V. (2016). The androgen receptor regulates pparγ expression and activity in human prostate cancer cells. *Journal of Cellular Physiology*, *231*(12), 2664–2672.

Piccinini, F. (2015). AnaSP: A software suite for automatic image analysis of multicellular spheroids. *Computer Methods and Programs in Biomedicine*, *119*(1), 43–52.

Rehberger, K., Kropf, C., & Segner, H. (2018). *In vitro* or not *in vitro*: a short journey through a long history. *Environmental Sciences Europe*, *30*(1), 23.

Riss, T. L., Moravec, R. A., Niles, A. L., Duellman, S., Benink, H. A., Worzlla, T. J., & Minor, L. (2013). Cell Viability Assays. In B. K. Sittampalam GS, Grossman A (Ed.), *Assay Guidance Manual*.

Rocha, E, Monteiro, R. A., & Pereira, C. A. (1994). The liver of the brown trout, *Salmo trutta fario*: a light and electron microscope study. *Journal of Anatomy*, *185*, 241–249.

Rocha, Eduardo, Monteiro, R. A. F., & Pereira, C. A. (1997). Liver of the brown trout, Salmo trutta (T*eleostei, Salmonidae*): A stereological study at light and electron microscopic levels. *Anatomical Record*, *247*(3), 317–328.

Rodd, A. L., Messier, N. J., Vaslet, C. A., & Kane, A. B. (2017). A 3D fish liver model for aquatic toxicology: Morphological changes and Cyp1a induction in PLHC-1 microtissues after repeated benzo(a)pyrene exposures. *Aquatic Toxicology*, *186*, 134–144.

Ruyter, B., Andersen, Ø., Dehli, A., Östlund Farrants, A. K., Gjøen, T., & Thomassen, M. S. (1997). Peroxisome proliferator activated receptors in Atlantic salmon (*Salmo salar*): Effects on PPAR transcription and acyl-CoA oxidase activity in hepatocytes by peroxisome proliferators and fatty acids. *Biochimica et Biophysica Acta - Lipids and Lipid Metabolism*, *1348*(3), 331–338.

Sahoo, P. K., Mohapatra, A., & Jena, J. K. (2017). Apolipoproteins in fish: From lipid transport to innate immunity. *Indian Journal of Animal Sciences*, *87*(6), 668–679.

Sakkiah, S., Wang, T., Zou, W., Wang, Y., Pan, B., Tong, W., & Hong, H. (2017). Endocrine disrupting chemicals mediated through binding androgen receptor are associated with diabetes mellitus. *International Journal of Environmental Research and Public Health*, *15*(1), 25.

Sargent, J., Tocher, D., & Bell, J. G. B. (2003). The Lipids. In *Fish nutrition*, 3,181–257.

Sato, K., Yoshinaka, R., Itoh, Y., & Sato, M. (1989). Molecular species of collagen in the

intramuscular connective tissue of fish. *Comparative Biochemistry and Physiology --
Part B: Biochemistry And*, *92*(1), 87–91.

Scaff, M., & Scussel, V. M. (2008). Ultra-structural and histochemical analysis of channel
catfish (*Ictalurus punctatus*) liver treated with fumonisin. *Brazilian Archives of Biology
and Technology*, *51*(2), 333–344.

Seglen, P. O. (1976). Preperation of isolated rat liver cells. In D. M. Prescott (Ed.),
Methods in Cell Biology, 13, 29–83).

Segner, H. (1998). Isolation and primary culture of teleost hepatocytes. *Comparative
Biochemistry and Physiology - A: Molecular and Integrative Physiology*, *120*, 71–81.

Segner, H., & Cravedi, J. (2001). Metabolic activity in primary cultures of fish hepatocytes
Metabolic activity in primary cultures of fish hepatocytes. *Alternatives to Laboratory
Animals: ATLA*, *29*, 251–257.

Shen, M., & Shi, H. (2015). Sex hormones and their receptors regulate liver energy
homeostasis. *International Journal of Endocrinology*, *2015*(294278), 1–12.

Singh, R., Artaza, J. N., Taylor, W. E., Gonzalez-Cadavid, N. F., & Bhasin, S. (2003).
Androgens stimulate myogenic differentiation and inhibit adipogenesis in c3h 10t1/2
pluripotent cells through an androgen receptor-mediated pathway. *Endocrinology*,
144(11), 5081–5088.

Sonneveld, E., Riteco, J. A. C., Jansen, H. J., Pieterse, B., Brouwer, A., Schoonen, W. G.,
& Burg, B. Van Der. (2006). Comparison of *in vitro* and *in vivo* screening models for
androgenic and estrogenic activities. *Toxicological Sciences*, *89*(1), 173–187.

Tocher, D. R. (2003). Metabolism and functions of lipids and fatty acids in teleost fish.
Reviews in Fisheries Science, *11*(2), 107–184.

Tokarz, J., Angelis, M., Adamski, J., & Möller, G. (2015). Steroids in teleost fishes : A
functional point of view. *Steroids*, *103*, 123–144.

Turchini, G. M., Torstensen, B. E., & Ng, W. K. (2009). Fish oil replacement in finfish
nutrition. *Reviews in Aquaculture*, *1*, 10–57.

Tzanakakis, E. S., Hansen, L. K., & Hu, W. (2001). The role of actin filaments and
microtubules in hepatocyte spheroid. *Cell Motility and the Cytoskeleton*, *48*, 175–189.

Uchea, C., Owen, S. F., & Chipman, J. K. (2015). Functional xenobiotic metabolism and
efflux transporters in trout hepatocyte spheroid cultures. *Toxicology Research*, *4*(2),
494–507.

Uchea, C., Sarda, S., Schulz-Utermoehl, T., Owen, S., & Chipman, K. J. (2013). *In vitro* models of xenobiotic metabolism in trout for use in environmental bioaccumulation studies. *Xenobiotica*, *43*(5), 421–431.

Urbatzka, R., Galante-Oliveira, S., Rocha, E., Lobo-da-Cunha, A., Castro, L. F. C., & Cunha, I. (2015). Effects of the PPARα agonist WY-14,643 on plasma lipids, enzymatic activities and mRNA expression of lipid metabolism genes in a marine flatfish, Scophthalmus maximus. *Aquatic Toxicology*, *164*, 155–162.

Van Roy, F., & Berx, G. (2008). The cell-cell adhesion molecule E-cadherin. *Cellular and Molecular Life Sciences*, *65*(23), 3756–3788.

Velasco-santamaría, Y. M., Korsgaard, B., Madsen, S. S., & Bjerregaard, P. (2011). Bezafibrate , a lipid-lowering pharmaceutical , as a potential endocrine disruptor in male zebrafish (*Danio rerio*). *Aquatic Toxicology*, *105*, 107–118.

Venkatachalam, A. B., Lall, S. P., Denovan-Wright, E. M., & Wright, J. M. (2012). Tissue-specific differential induction of duplicated fatty acid-binding protein genes by the peroxisome proliferator, clofibrate, in zebrafish (*Danio rerio*). *BMC Evolutionary Biology*, *12*(112), 1471–2148.

Vluggens, A., Andreoletti, P., Viswakarma, N., Jia, Y., Matsumoto, K., Kulik, W., Khan, M., Huang, J., Guo, D. Sangtao Yu, S., Rao, J. M. S., Wanders, R. J., Reddy, J. K. & Cherkaoui-Malki, M. (2010). Functional significance of the two ACOX1 isoforms and their crosstalks with PPARα and RXRα. *Laboratory Investigation*, *90*(5), 696–708.

Vosough, M., Omidinia, E., Kadivar, M., Shokrgozar, M.-A., Pournasr, B., Aghdami, N., & Baharvand, H. (2013). Generation of functional hepatocyte-like cells from human pluripotent stem cells in a scalable suspension culture. *Stem Cells and Development*, *22*(20), 2693–2705.

Walzl, A., Unger, C., Kramer, N., Unterleuthner, D., Scherzer, M., Hengstschläger, M., Schwanzer-Pfeiffer, D. & Dolznig, H. (2014). The resazurin reduction assay can distinguish cytotoxic from cytostatic compounds in spheroid screening assays. *Journal of Biomolecular Screening*, *19*(7), 1047–1059.

Wang, G., Bonkovsky, H. L., Lemos, A. De, & Burczynski, F. J. (2015). Recent insights into the biological functions of liver fatty acid binding protein *1. Journal of Lipid Research. 56*, 2238–2247.

Wang, X., Yu, X., & Tong, J. (2016). Molecular characterization and growth association of two apolipoprotein A-Ib genes in common carp (*Cyprinus carpio*). *International*

Journal of Molecular Sciences, *17*(1569), 1–14.

Wolfrum, C., Borrmann, C. M., Börchers, T., & Spener, F. (2001). Fatty acids and hypolipidemic drugs regulate peroxisome proliferator-activated receptors α- and γ-mediated gene expression via liver fatty acid binding protein: A signaling path to the nucleus. *Proceedings of the National Academy of Sciences of the United States of America*, *98*(5), 2323–2328.

Young, G., Kusakabe, M., Nakamura, I., Lokman, P. M., & Goetz, F. W. (2005). Gonadal Steroidogenesis in Teleost Fish. *Hormones and Their Receptors in Fish Reproduction*, 155–223.

Zanoni, M., Piccinini, F., Arienti, C., Zamagni, A., Santi, S., Polico, R., Bevilacqua, A. & Tesei, A. (2016). 3D tumor spheroid models for *in vitro* therapeutic screening: A systematic approach to enhance the biological relevance of data obtained. *Scientific Reports*, *6*, 1–11.

Zhao, Y., Zhang, K., Giesy, J. P., & Hu, J. (2015). Families of nuclear receptors in vertebrate models: characteristic and comparative toxicological perspective. *Scientific Reports*, *5*(8554), 1–9.

Zheng, J. L., Luo, Z., Zhu, Q. L., Tan, X. Y., Chen, Q. L., Sun, L. D., & Hu, W. (2013). Molecular cloning and expression pattern of 11 genes involved in lipid metabolism in yellow catfish *Pelteobagrus fulvidraco. Gene*, *531*(1), 53–63.

Appendix A — Preparation of Buffers and Stock Solutions for Hepatocyte Isolation

Preparation of stock solutions per fish:

Stock 1 – Dissolve 8.0 g of sodium chloride (NaCl) and 0.4 g of potassium chloride (KCl) in a total of 100 mL of distilled water.

Stock 2 – Dissolve 0.358 g of sodium phosphate dibasic (Na_2HPO_4) and 0.6 g of potassium phosphate monobasic (KH_2PO_4) in a total of 100 mL of distilled water.

Stock 3 – Dissolve 0.72 g of calcium chloride ($CaCl_2$) in 50 mL of distilled water.

Stock 4 – Dissolve 1.23 g of magnesium sulphate heptahydrate ($MgSO_4$ x $7H_2O$) in 5 mL of distilled water.

Stock 5 – Dissolve 0.35 g of sodium bicarbonate ($NaHCO_3$) in 10 mL of distilled water.

Preparation of isolation buffers per fish:

Buffer 1 (50 mL): Mix 5 mL of stock1 + 0.5 mL of stock2 + 8 mL of distilled water + 0.5 mL of stock4 + 0.5 mL of stock5 + 10 mM of ethylenediamine tetraacetic acid (EDTA)

> **Preparation of 10 mM EDTA:** 35 mL distilled water + 0.146 g EDTA. This solution was only prepared 1 day before hepatocyte isolation, and added on the isolation day, followed by adjustment of the buffer's pH to 7.9 – 8.0.

Buffer 2 (30 mL): Mix 3 mL of stock1 **+** 0.3 mL of stock2 **+** 0.3 mL of stock3 **+** 25.8 mL of distilled water **+** 0.3 mL of stock4 **+** 0.3 mL of stock5 **+** 0.05% of collagenase. The pH was adjusted to 7.2 – 7.4.

> **Preparation of 0.05% collagenase:** 15 mg of collagenase (Sigma-Aldrich) were stored at -20 ºC and added on the moment of its use.

Buffer 3 (200 mL): Mix 20 mL of stock1 **+** 2 mL of stock2 **+** 2 mL of stock3 **+** 172 mL of distilled water **+** 2 mL of stock4 **+** 2 mL of stock5. The pH was adjusted to 7.2 – 7.4.

Appendix B   – 2D Trypan Blue protocol

1. Aspirate the medium from the wells
2. Wash two to three times with 500 µL sterile PBS (Sigma-Aldrich)
3. Apply 150 µL of trypsin/EDTA (0.05%/0.02%, Sigma-Aldrich) in PBS for 5 min
4. Verify cell detachment under microscope
5. Stop the action of trypsin with 300 µL of Leibovitz's L-15 supplemented medium
6. Aspirate cell suspension to a 1.5 mL Eppendorf
7. Homogenize and prepare a 1:1 dilution - 10µL of cellular suspension and 10µL of Trypan Blue 0.1% (Invitrogen). Re-suspend and insert the mixture in cell countess cassettes
8. Asses viability, amount of living, dead and total cells/mL by inserting the cassette in the CountessTM Automated Cell Counter.

Appendix C   **– Hematoxylin and Eosin (H&E) Staining Protocol for Paraffin Sections**

1. Deparaffinize with xylene (VWR) (2 x 10 min);
2. Hydrate in a graded series of ethanol (100%; 95%; 70%) for 5 min each;
3. Wash in running tap water (5 min);
4. Stain nuclei with commercial Mayer's Hematoxylin (Merck) for 2 min;
5. Wash in running tap water (5 min);
6. Stain with aqueous 1% Eosin (Bio-Optica) for 2 - 4 min;
7. Quickly wash in tap water;
8. Dehydrate three times in ethanol 99.9%;
9. Clear in xylene (2 min each);
10. Mount with Q Path® Coverquick 2000 media (VWR).

Appendix D — Periodic Acid Schiff (PAS) Staining and PAS with Diastase Protocols for Paraffin Sections

1. Deparaffinize and hydrate the sections;
2. Oxidize with Periodic Acid Solution 0,5% (ThermoFischer Scientific) for 15 min;
3. Wash in running tap water for 5 min;
4. Pass through distilled water;
5. Cover the sections with Schiff's Reagent (ThermoFischer Scientific) for 20 min;
6. Wash in running tap water for 5 min;
7. Nuclei staining with Mayer's Hematoxylin for 1 min;
8. Wash in running tap water for 5 min;
9. Dehydrate, clear with xylene and mount.

PAS with diastase protocol:

1. Deparaffinize and hydrate the sections;
2. Digest with alfa-amylase 0,5% (Sigma-Aldrich) for 30 min at 37 ºC;
3. Wash in tap water for 5 min;
4. Continue from step 2. of the PAS protocol.

Appendix E   **– Masson's Trichrome Staining Protocol for Paraffin Sections**

1. Deparaffinize and hydrate the sections;
2. Incubate the slides in Bouin's Solution (VWR) at 60 ºC for 1h;
3. Wash in tap water;
4. Cover the sections in Celestine Blue (Sigma-Aldrich) for 5 min;
5. Wash in distilled water for 5 min;
6. Incubate in Mayer's Hematoxylin for 2 min;
7. Wash in tap water for 5 min;
8. Stain with the Ponceau Xylidine / Acid Fuchsin mix for 5 min;
9. Wash in distilled water;
10. Cover the sections with 1% Phosphomolybdic Acid for 5 min;
11. Clear the slide (simply by letting the acid drain from the slides);
12. Stain with Aniline blue for 2 – 5 min;
13. Differentiate by spraying 1% acetic acid;
14. Wash in distilled water;
15. Dehydrate, clear with xylene and mount.